ELSEVIER

Journal of Structural Geology 29 (2007) 1585–1604

JOURNAL OF STRUCTURAL GEOLOGY

www.elsevier.com/locate/jsg

Scale invariant sheath folds in salt, sediments and shear zones

G.I. Alsop [a,*], R.E. Holdsworth [b], K.J.W. McCaffrey [b]

[a] *Crustal Geodynamics Group, School of Geography & Geosciences, University of St. Andrews, Fife, KY16 9AL, UK*
[b] *Reactivation Research Group, Department of Earth Sciences, University of Durham, Durham, DH1 3LE, UK*

Received 21 March 2007; received in revised form 6 July 2007; accepted 17 July 2007
Available online 31 July 2007

Abstract

Sheath folds are developed in a broad spectrum of geological environments in which material flow occurs, including gravity-driven surficial deformation in ignimbrites, unconsolidated sediments and salt, together with deeper level ductile shear zones in metamorphic rocks. This study represents the first geometric comparison of sheath folds in these different settings across a wide range of scales. Elliptical closures defining eye-folds represent (y–z) cross sections through highly-curvilinear sheath folds. Our analysis of the published literature, coupled with field observations, reveals remarkably similar ellipticities (R_{yz}) for sheath folds in metamorphic shear zones (R_{yz} 4.23), salt (R_{yz} 4.29), sediment slumps (R_{yz} 4.34), glaciotectonites (R_{yz} 4.48), and ignimbrites (R_{yz} 4.34). Nested eye-folds across this range of materials ($N = 1800$) reveal distinct and consistent differences in ellipticity from the outer- (R_{yz}) to the inner-most ($R_{y'z'}$) elliptical ''rings'' of individual sheath folds. The variation in ratios from outer to inner rings ($R' = R_{yz}/R_{y'z'}$) in gravity-driven surficial flows typically displays a relative increase in ellipticity to define cats-eye-folds ($R' < 1$) similar to those observed during simple and general shear in metamorphic rocks. We show that sheath folds develop across a range of scales within these different environments, and display elliptical ratios (R_{yz}) that are remarkably constant ($R^2 > 0.99$) across 9 orders of magnitude (sheath y axes range from ~0.1 mm to >75 km). Our findings lead us to conclude that the geometric properties of sheath folds are scale invariant and primarily controlled by the type and amount of strain, with R' also reflecting the rheological significance of layering associated with original buckle fold mechanisms. The scaling pattern of sheath folds reflects the length scales of the precursor buckle folds (and width of deformation zones) across a broad range of materials and environments. With continued deformation, the layering marking the original folds may become increasingly passive to define sheath folds. These empirical relationships suggest sheath folding is a fundamental mode of viscous response across a broad spectrum of materials, strain rates and scales encompassing a variety of deformation settings.

Keywords: Sheath folds; Shear zones; Deformation; Flow perturbations; High strain; Progressive deformation

1. Introduction

Sheath folds are increasingly recognised in high-strain zones across a broad range of geological settings and environments including mid-crustal shear zones (see Alsop and Holdsworth, 2004a,b), salt diapirs and flows (e.g. Talbot and Jackson, 1987; Davison et al., 1996; Alsop et al., 2000), soft-sediment slump sheets (e.g. Roberts, 1989; Strachan and Alsop, 2006), sub-glacially sheared sediment (e.g. Van der Wateren, 1999) and ignimbrite flows (e.g. Branney et al., 2004). The dimensions of recorded sheath folds may vary through several orders of magnitude in each of these settings. In addition sheath folds have also been recorded from ice sheets (e.g. Hudleston, 1992; Goodsell et al., 2002), from syn-magmatic slumps within layered igneous complexes (e.g. Clarke et al., 2005) and on the sub-millimetre scale within flow patterns associated with injection of pseudotachylyte veins (e.g. Berlenbach and Roering, 1992; Theunissen et al., 2002; Rowe et al., 2005) and tremolitic glass (e.g. Shao et al., 1989). They have also been described from within shallowly-buried inter-bedded coals and shales upon which gravity has operated (e.g. Wang et al., 1994). Sections through sheath-like tongues of pahoehoe lava have also been recorded (e.g. Guilbaud et al., 2005) and result in classic

* Corresponding author.
E-mail address: gia@st-andrews.ac.uk (G.I. Alsop).

0191-8141/$ - see front matter © 2007 Elsevier Ltd. All rights reserved.
doi:10.1016/j.jsg.2007.07.012

elliptical or eye-shaped closures. Sheath folds have been described from Quaternary sediments whilst the oldest dated sheath is defined by an intensely folded tonalite sheet that yields an age of 3640 Ma within the Palaeoarchean of Greenland (Hanmer et al., 2002).

Sheath folds form a specific sub-group of highly curvilinear folds with hinge-line angles varying through >90°. They are typically considered to form in high strain zones due to the sequential rotation of fold hinges that initiate at high angles to the direction of shear during progressive non-coaxial deformation (Cobbold and Quinquis, 1980). Gentle curvilinearity of the initial fold hinge is generally believed to be accentuated during subsequent shearing to create highly curvilinear structures. Despite the apparent ubiquity and scale range exhibited by sheath folds developed within a wide range of geological environments involving material flow, there are no published comparative studies or detailed analyses of their geometric properties. This study presents the first systematic and comprehensive geometric analysis of sheath folds developed across a broad range of differing lithologies, settings, strain rates and scales. It will thus help identify and constrain fundamental deformation processes operating across such a range of scales and environments.

2. Analysis of sheath folds

Sheath folds are best described with reference to a simple Cartesian reference frame. An x axis can be defined lying along the length of the tube or tongue, whilst cross sections normal to the x axis display elliptical eye-folds whose long and short axes lie parallel to the y and short z axes, respectively (Fig. 1a). The x, y and z geometric axes of sheath folds are typically considered to lie sub-parallel to the X, Y and Z axes of the finite strain ellipsoid (e.g. Quinquis et al., 1978; Minnigh, 1979). The x axis of the sheath fold is thus considered to be broadly parallel with the mineral elongation lineation (X), which marks the transport direction during intense non-coaxial deformation, whilst the sheath y axis lies in the axial plane (X–Y surface) with the z axis forming the normal to that plane.

In order to obtain reliable and consistent y–z ratios associated with elliptical eye-folds, sections across the apex (nose) of the outer-fold should be avoided as this will contain only limited internal elliptical patterns (nested closures), whilst the base of the fold will be complicated and influenced by the onset of double-vergence geometries. Our analysis of the published literature concerning serially sectioned sheaths (e.g. Minnigh, 1979; Crispini and Capponi, 1997), together with our own observations, suggest that this nose region comprises <20% of the length of the sheath x axis. Viewed sections should thus avoid the apex (marked by limited internal ellipses) and base (marked by double vergence) of the outer-fold and cut directly across the main body of the sheath (see Alsop and Holdsworth, 2006 for details). We have measured the intermediate (y) and short (z) axes from sheath fold eye-shaped cross-sections using a variety of sources including photographs, maps and plans. These published data were analysed as they clearly illustrate completely closed, nested elliptical patterns and lack of double-vergence geometries noted above. Although most authors specifically state that photos of

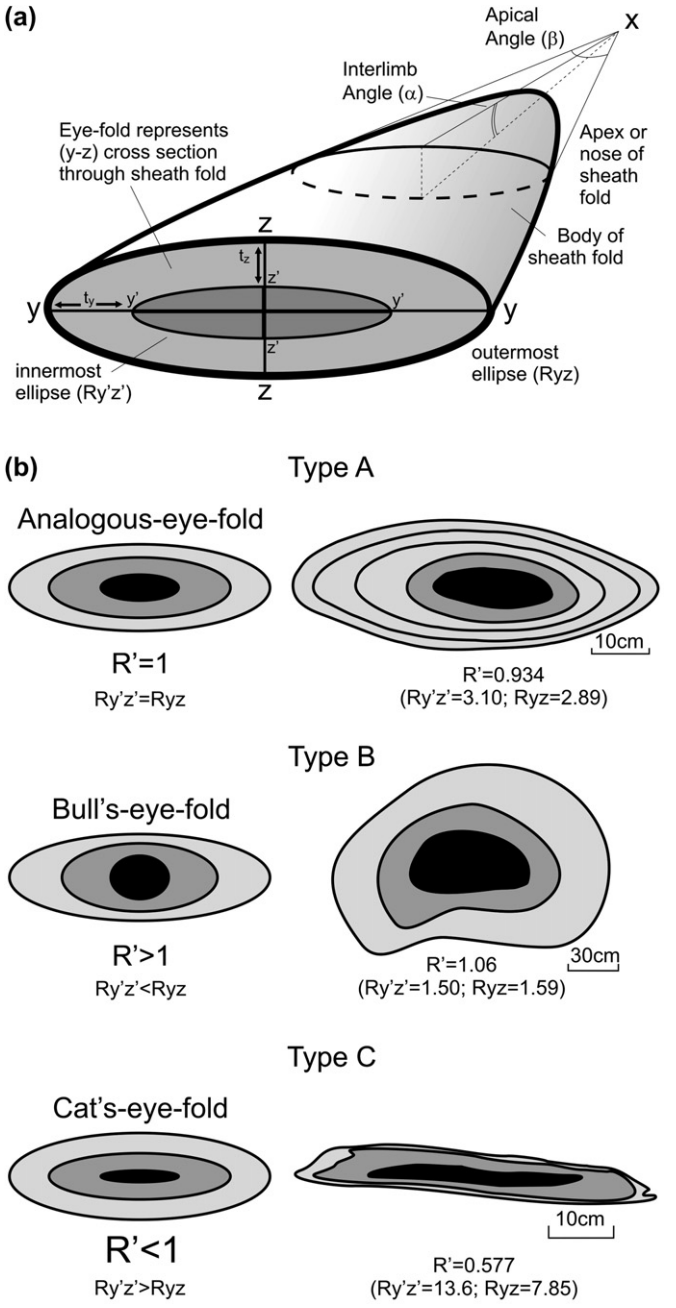

Fig. 1. (a) Schematic diagram illustrating the x, y and z axes of a sheath fold together with the inter-limb angle (α) and apical angle (β) of the curvilinear fold hinge-line. Elliptical ratios of the outermost ring (R_{yz}) and innermost ring ($R_{y'z'}$) are also given. Y–Z orientated cross sections across the sheath fold result in eye-fold geometries. Elliptical ratios of the outermost ring (R_{yz}) and innermost ring ($R_{y'z'}$) are also given. The thickness of any individual layer may be measured along the y axis (t_y) and at 90° to this along the z axis (t_z) to provide a ratio (T_{yz}) of layer thickening/thinning. (b) Schematic diagram illustrating the variation in elliptical ratios (R') within Type A, analogous-eye-fold (R' 1), Type B, bulls-eye-fold (R' >1) and Type C, cats-eye-fold (R' <1). Down-plunge sketches illustrate typical examples of sheath folds developed in metamorphic rocks displaying analogous-eye-fold (Hansen, 1971), bulls-eye-fold (Kelly et al., 2000), and cats-eye-fold patterns (Harms et al., 2004).

eye-folds are taken looking down the transport (X) direction, in some cases the cross-sectional view may be oblique to the Cartesian reference frame. Clearly the hinges of sheath folds lie sub-parallel to the mineral lineation (X) which typically

bisects the nose of the fold, and this may be used as an approximation for restoring the plunge of the sheath x axis. The axial (x–y) planes of sheath folds will form sub-parallel to the foliation. Thus, simple calculations have been made when necessary to correct for plunging hinges and inclined axial surfaces. Dome and basin interference patterns generated by refolding and polyphase folding are excluded from our data set.

Nested closures defining eye-folds may display consistent differences in ellipticity from the outer- (R_{yz}) to the inner-most ($R_{y'z'}$) eye-shaped rings of individual sheath folds (Fig. 1a) (Alsop and Holdsworth, 2006). The outer-most ellipse (R_{yz}) may be defined as the largest complete elliptical ring which is observed. It is normally bounded on the outer margin by a surface which displays incomplete elliptical closures characterised by double-vergence geometries. The inner-most elliptical ring ($R_{y'z'}$) forms the smallest observed elliptical pattern situated within the outer-most ellipse. The variation in overall aspect ratios from outer to inner rings of eye-folds is defined as R' (where $R' = R_{yz}/R_{y'z'}$) and may display Type A or analogous-eye-fold (R' 1), Type B or bulls-eye-fold ($R' > 1$) or Type C and cats-eye-fold ($R' < 1$) geometries (Fig. 1b). From an analysis of sheath folds developed within metamorphic shear zones, Alsop and Holdsworth (2006) have shown that more than 98% of sheath folds formed during simple or general shear (see Simpson and De Paor, 1993 for definitions) display cats-eye-fold geometries ($R' < 1$). By contrast, >90% of sheaths generated during constriction (associated with shortening along both the Y and Z axes) display bulls-eye-fold geometries ($R' > 1$). Criteria used to distinguish the different deformation regimes are fully explained by Alsop and Holdsworth (2006). Layer thicknesses may also be measured along the y axis (parallel to the axial surface) (t_y) and at 90° to this along the z axis (t_z) to define the ratio of T_{yz} (Fig. 1a). This ratio displays a progressive increase from sheaths developed during constriction (T_{yz} 2.94), simple shear (T_{yz} 3.31), and general shear (T_{yz} 4.35) deformation. The empirical relationships and correlations noted above led Alsop and Holdsworth (2006) to suggest that the nature of simple shear, general shear or constrictional deformation imposes fundamental constraints on the geometry of sheath folds within metamorphic rocks.

The present study builds on the descriptive framework established by Alsop and Holdsworth (2006) and extends the concept of eye-fold analysis into different metamorphic rock types, together with a variety of new environments associated with gravity-driven flows. In addition we also now extend the analysis of sheaths through several orders of magnitude into major (kilometre scale) structures. In this study, we have investigated eye-folds from a range of geological settings and materials and across 9 orders of magnitude in an attempt to address fundamental questions concerning the variation in sheath fold geometry with host material type, strain rate and scale.

3. Does sheath fold geometry vary with material and environment?

We have measured and analysed more than 1800 nested eye-folds representing y–z eye-shaped cross sections through sheaths, combining our own measurements with data taken from publications covering a range of geological settings and materials (Figs. 2, 3). These include sheath folds in metamorphic shear zones, salt diapirs, unlithified ‘‘soft’’ sediment deformation and slumps, glaciotectonised sediments, ignimbrite flows, laboratory models, pseudotachylytes and ice.

3.1. Sheath folds within metamorphic rocks

Most detailed studies into the mechanisms and generation of sheath folds have focussed predominantly upon metamorphic rocks (e.g. Carreras et al., 1977; Quinquis et al., 1978; Minnigh, 1979). Such studies typically demonstrate an association of sheath folds with intense non-coaxial deformation, marked by the tectonic transport direction bisecting the arc of fold hinge curvature (see Alsop and Holdsworth, 2004a,b, 2005 and references therein). Recent numerical studies by Kuiper et al. (2007) suggest that in some extreme cases of general shear it may be theoretically possible for sheath folds to develop oblique to the mineral lineation, although such scenarios appear uncommon in nature.

Sheath folds developed within metamorphic rocks display elliptical ratios that typically vary between 1 and 15, with the majority in the range of 2–5 (Fig. 4a, Table 1). In detail, the outer ellipses display lower ratios (R_{yz}) than the inner ellipses ($R_{y'z'}$) leading to cats-eye-fold shapes (Figs. 1b, 4b, Table 1). Outer and inner elliptical ratios of individual sheath folds are directly compared on eye-charts where they display a distinct trend reflecting the overall cats-eye-fold patterns associated with simple/general shear (Fig. 5a). Bulls-eye-fold patterns are only developed with low ($R_{yz} < 3$) elliptical ratios and are generally associated with constrictional deformation (Fig. 1b) (Alsop and Holdsworth, 2006).

Many previous studies have suggested that lithology may play an important role in the development of folds (e.g. see Ramsay, 1967; Ramsay and Huber, 1987). In order to specifically assess the role of lithological variation on the generation and evolution of sheath folds, a study of sheath geometry in some of the major metamorphic rock types has been undertaken. These include quartzite, carbonate, psammite (± pelite), gneiss (± amphibolite) (Table 2). Clearly, these broad groupings are based on predominant rock types and may include some thin layers and minor components, e.g. pelite within psammite, which will induce local and perhaps sometimes significant competency contrasts. Criteria used by original authors to independently determine the nature of simple shear, general shear or constrictional deformation associated with sheath folding are discussed by Alsop and Holdsworth (2006). It is important to note that most authors typically employ a combination of criteria when assigning bulk deformation types.

In both simple shear and general shear, the most pronounced ellipses with more extreme $R_{y'z'}$ aspect ratios and lower R' values are displayed by sheath folds developed within carbonates and quartzites (Table 2). Conversely, lower $R_{y'z'}$ values combined with greater R' magnitudes are displayed by sheaths developed within gneisses and psammites. During general shear, sheath folds within quartzite tend to plot with lower R' for any given $R_{y'z'}$ value, indicating a greater difference in aspect ratio between

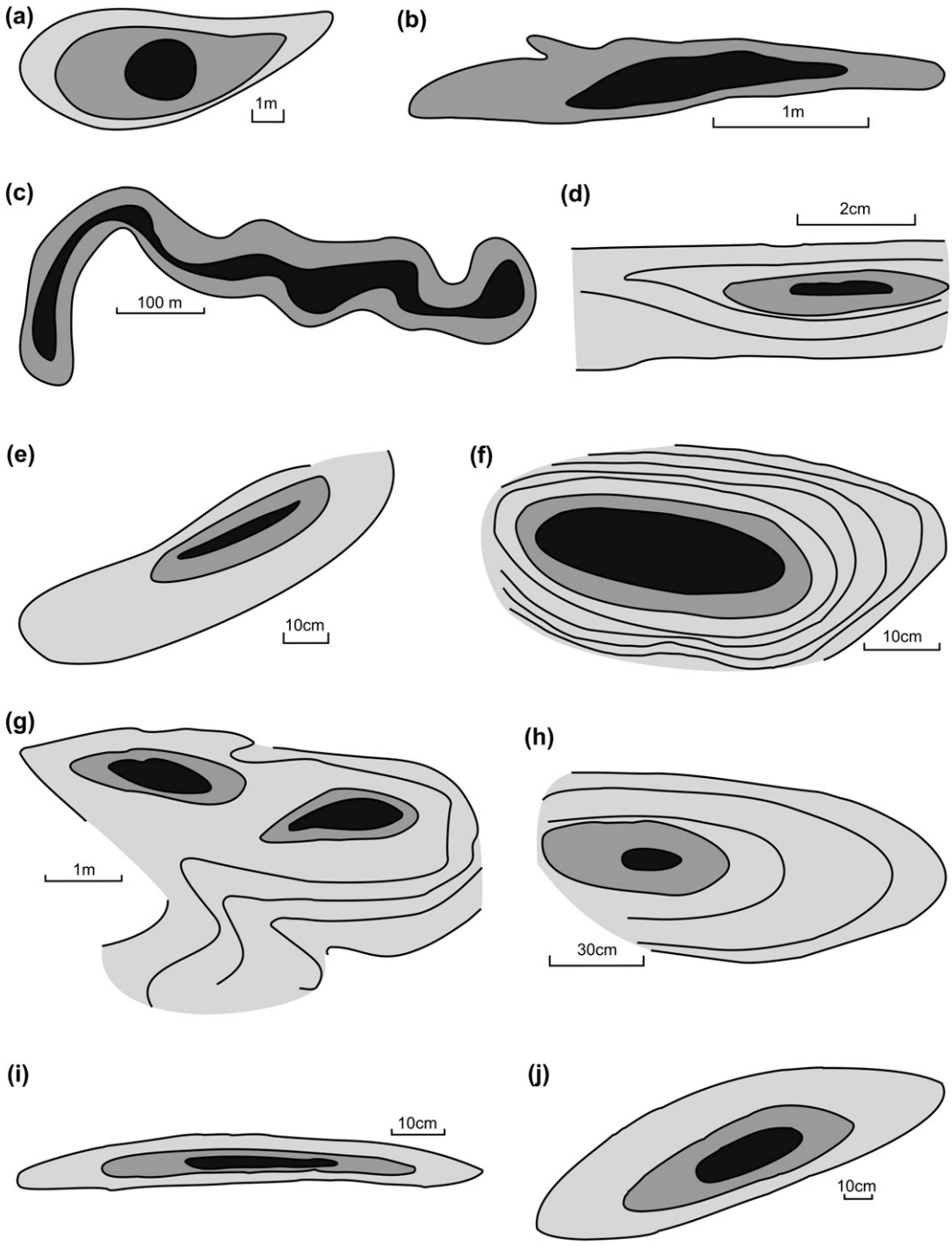

Fig. 2. Line drawings from photographs and sketches of sheath folds in different materials including salt (a–d), sediment slumps (e,f), glaciotectonised sediment (g,h), and rheomorphic ignimbrites (i,j). Eye-folds represent y–z cross sections through sheath folds (see Fig. 1) with illustrations being based on (a) Balk, 1949. (b) Muehlberger and Clabaugh, 1968. (c) Talbot and Koyi, 1998. (d) Carter, 1990c. (e) Hibbard and Karig, 1987. (f) Sarr et al., 2000. (g) Van der Wateren et al., 2000. (h) Van der Wateren, 1999. (i,j) Branney et al., 2004.

the outer and inner ellipses defining cats-eye-folds. During constriction, sheath folds within carbonate and quartzite display greater R' values associated with extremely low ($R_{y'z'}$) aspect ratios when compared with those in psammite. Within each analysed lithology, sheath folds display a progression in layer thickness (T_{yz}) ratios around the fold from those generated during constrictional deformation through simple shear sheaths to the greatest T_{yz} values recorded during general shear (Table 2). In summary, sheath folds developed in quartzite and carbonate typically display the most extreme variations in elliptical ratios and R' values, when compared to those in psammite and gneiss. This relationship may be interpreted as reflecting the greater susceptibility of quartzites and carbonates to flow associated with ductile deformation (e.g. see Ramsay, 1982).

Fig. 3. 3-D exposures of highly curvilinear soft-sediment sheath folds that display more than 90° of hinge-line variation exposed in carboniferous sandstones and mudstones of the Fisherstreet Slump in County Clare, Ireland (see Strachan and Alsop, 2006). The recumbent fold is tight to isoclinal and displays pronounced hinge-line curvature around the nose of the sheath. Hammer is placed towards the nose of the fold.

3.2. Sheath folds within salt

Sheath folds are most widely reported from within diapiric salt, where eye-shaped closure patterns have long been recognised in the galleries of salt mines (e.g. Balk, 1949, 1953; Hoy et al., 1962; Kupfer, 1962, 1976; Talbot and Jackson, 1987) (Fig. 2a,b,c,d), from reconnaissance aerial photography of salt domes (e.g. Kent, 1970), and also generated within paraffin and clay physical models of salt diapirs (e.g. Escher and Kuenen, 1929). Analyses of aerial photographs and maps of salt diapirs from the Great Kavir of Central Iran reveal numerous eye-fold patterns which are considered sheath-like and indicative of extreme ductile strains (Jackson et al., 1990 (pp. 56, 57). Cross sections through the elliptical closures within the diapirs display dominantly cats-eye patterns. Sheath folds and associated eye-structures are also typically developed along detachments within relatively weak salt and evaporitic units undergoing regional folding and thrusting (e.g. Marcoux et al., 1987; Harland et al., 1988; Malavieille and Ritz, 1989; Sans et al., 1996), together with lateral salt flows (Talbot and Koyi, 1998) (Fig. 2c).

Sheath folds in salt display elliptical ratios varying from 1 to 15, but more typically in the range 2–6 (Fig. 4c, Table 1). Overall, 90% of analysed sheath folds within salt display cats-eye patterns (Figs. 4d, 5a) with remarkably similar thickness (T_{yz}) ratios to those recorded in quartzite and carbonate during simple shear (Tables 1, 2). Minor components (~7%) of bulls-eye and analogous-eye (~3%) fold patterns also occur within salt with thickness ratios (T_{yz} 2.445) similar to those recorded in sheath folds developed in quartzite and gneiss during constrictional deformation. The overall mean values for sheath folds developed in salt are R_{yz} 5.1, R' 0.783 and T_{yz} 3.023 (Table 1).

3.3. Sheath folds within soft sediment slumps

Highly curvilinear ‘‘double-verging’’ folds and sheath folds marked by extreme fold hinge thickening are associated with soft-sediment deformation in a number of settings. These include accretionary complexes (Fig. 2e) (e.g. Hibbard and Karig, 1987; Agar, 1988; George, 1990), oceanic transform margins (e.g. Benkhelil et al., 1998), thrusting of poorly lithified sediments (e.g. Nigro and Renda, 2004), together with sediment slump sheets (Figs. 2f, 3) (e.g. McBride, 1962; Blatt et al., 1980; Allen, 1982; Faure, 1985; Ghosh and Mukhopadhyay, 1986; Farrell and Eaton, 1987, 1988; Webb and Cooper, 1988; Roberts, 1989; Eyles et al., 1989; Decker, 1990; Maltman, 1994; Smith, 2000; Sarr et al., 2000). Sheath folds within such settings may be marked by ‘‘tongues’’ of sediment produced by local differential movement within the slump sheet, whereas others are typically found in association with decollements marked by simple-shear dominated deformation. Similar variability in folding possibly related to perturbations in flow has also been suggested in mid-crustal shear zones (e.g. Alsop and Holdsworth, 1993, 2002, 2004c and references therein; Alsop et al., 1996). In addition, it has been demonstrated that concepts of minor fold vergence, facing and obliquity to transport largely applied to folds within mid-crustal deformation may be successfully employed in the analysis of such slumps (e.g. Roberts, 1989; Strachan and Alsop, 2006).

Sheath fold eyes formed in sedimentary slumps typically display elliptical ratios between 3 and 6 (mean 5.25), with few sheaths developing ratios >8 (Fig. 4e, Table 1). The outer ellipses display lower ratios (R_{yz} 4.34) than the inner ($R_{y'z'}$ 6.28) (Fig. 4f) resulting in cats-eye-fold patterns on eye-charts

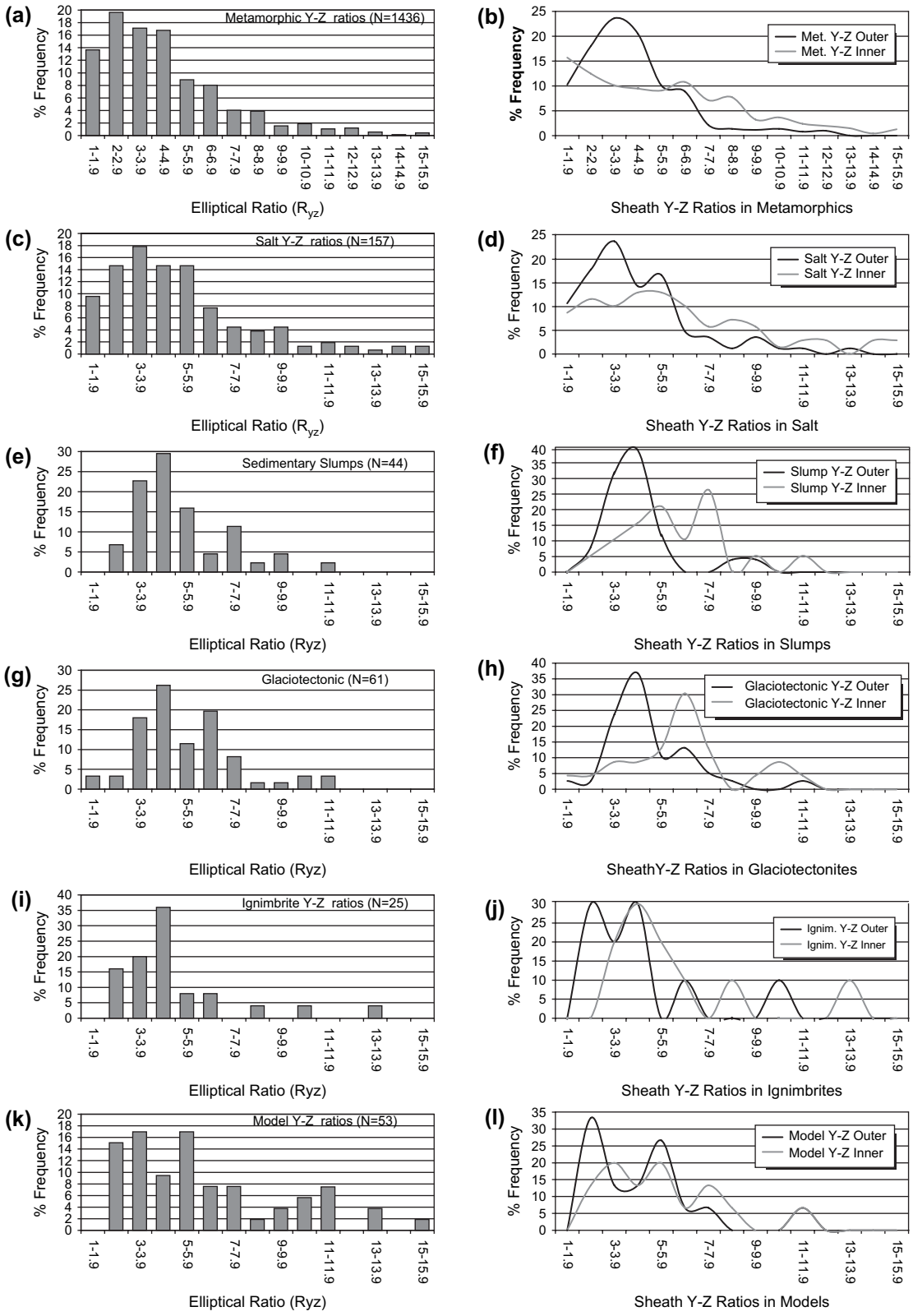

Fig. 4. % Frequency histograms and distribution curves for inner and outer elliptical ratios (R_{yz}) of sheath folds from (a,b) metamorphic shear zones ($N = 1436$). See Alsop and Holdsworth (2006) and references therein for data sources. (c,d) Salt flows ($N = 157$). Data analysed from Balk (1949, 1953), Hoy et al. (1962), Kupfer (1962, 1976), Muehlberger and Clabaugh (1968), Talbot and Jackson (1987), Carter (1990a,b,c), Jackson et al. (1990), Roberts and Williams (1993), Burliga (1996), Talbot and Koyi (1998), Talbot and Aftabi, 2004. (e,f) Soft-sediment slumps ($N = 44$). Data analysed from McBride (1962), Allen (1982), Blatt et al. (1980), Ghosh and Mukhopadhyay (1986), Van der Pluijm (1986), Hibbard and Karig (1987), Decker (1990), Maltman (1994), Bradley and Hanson (1998), Sarr et al. (2000), Schoonver and Osozawa (2004). (g,h) Glaciotectonised sediment ($N = 61$). Data analysed from Banham and Ranson (1965), Thomas (1984), Owen (1988), Owen and Derbyshire (1988), Eyles et al. (1989), Kluiving et al. (1991), Matoshko (1995), Van der Wateren (1999), Van der Wateren et al. (2000), Pedersen (2000), Bennett et al. (2000, Lian et al. (2003), Benediktsson (2005), Cox (2006), Möller (2006). (i, j) Ignimbrite flows ($N = 25$). Data analysed from Branney et al. (2004). (k,l) Models ($N = 53$). Data analysed from Cobbold and Quinquis (1980), Mulugeta and Koyi (1987), Brun and Merle (1988), Jackson and Talbot (1989), Jackson et al. (1990).

Table 1
General parameters of sheath folds in different materials

	Metamorphics ($N = 1462$ from 518 sheaths)	Salt ($N = 157$ from 84 sheaths)	Slumps ($N = 52$ from 26 sheaths)	Glaciotectonites ($N = 68$ from 27 sheaths)	Ignimbrites ($N = 25$ from 10 sheaths)	Models ($N = 53$ from 38 sheaths)
Scale (y axes)	0.1 mm–75 km	1 m–13 km	5.9 mm–27 m	70 mm–80 m	5.8 cm–5.9 m	1.8 mm–38 mm
Scale (z axes)	0.04 mm–20 km	162 mm–1522 m	0.8 mm–9 m	23 mm–20 m	11 mm–1.8 m	0.2 mm–5.8 mm
Orders of magnitude (mm)	9 (10^{-1} to 10^{8})	4 (10^{3} to 10^{7})	4 (10^{0} to 10^{4})	4 (10^{1} to 10^{5})	2 (10^{1} to 10^{3})	1 (10^{0} to 10^{1})
Outer ellipse ratio	$y = 1.037x - 0.7$	$y = 1.017x - 0.72$	$y = 1.077x - 0.84$	$y = 1.012x - 0.73$	$y = 1.065x - 0.82$	$y = 0.755x - 0.51$
R^2	0.987	0.995	0.992	0.959	0.991	0.936
Inner-outer elliptical ratios	y=0.55x+0.99	$y = 0.57x + 0.79$	$y = 0.5362x + 0.9969$	$y = 0.508x + 1.2762$	$y = 0.87x - 0.79$	$y = 0.86x$
R^2	0.9172	0.9042	0.7877	0.8633	0.9787	0.9446
Mean R_{y-z} (outer ellipse)	4.227	4.287	4.339	4.476	4.338	4.149
Mean $R_{y'-z'}$ (inner ellipse)	5.901	6.143	6.276	6.298	5.8965	5.2528
Mean R_{y-z} (overall)	4.827	5.138	5.245	5.369	4.87	6.39
Mean R'	0.8485	0.7833	0.710	0.738	0.713	0.8156
Mean T_{yz}	3.312	3.023	3.158	3.276	3.123	3.230
Strain rate	10^{-15} to 10^{-13} s^{-1}	10^{-8} s^{-1}	10^{-7} s^{-1}	10^{-7} s^{-1}	10^{2} to 10^{4} s^{-1}	Variable

(Fig. 5a, Table 1). Overall, sheath folds formed in sedimentary slumps display (100%) cats-eye-folds marked by mean R' 0.710, R_{yz} 5.25 and T_{yz} 3.158 (Table 1).

3.4. Sheath folds within glaciotectonised sediment

A large number of authors have observed well-developed metre scale sheath folds and eye-structures generated during intense deformation of unlithified sub-glacial tills (Fig. 2g,h) (e.g. Banham and Ranson, 1965; Thomas, 1984; Owen, 1988; Owen and Derbyshire, 1988; Kluiving et al., 1991; Matoshko, 1995; Van der Wateren, 1999; Pedersen, 2000; Van der Wateren et al., 2000; Bennett et al., 2000; Lian et al., 2003; Piotrowski and Windelberg, 2003; Benediktsson, 2005; Cox, 2006; Möller, 2006) and also within drumlins (Hart, 1997). The nature of fabrics developed during sub-glacial shearing has been highlighted by Van der Wateren et al. (2000). They propose that simple shear is the predominant style of deformation within glaciotectonised sediments.

Sheath folds formed in glaciotectonised sediments typically display elliptical ratios between 3 and 7, with few sheaths developing ratios >8 (Fig. 4g, Table 1). The outer ellipses display lower ratios (R_{yz} 4.48) compared to the inner ellipses ($R_{y'z'}$ 6.30) (Figs. 4h, 5a, Table 1). Overall, sheath folds formed in glaciotectonised sediments display predominantly (>95%) cats-eye patterns marked by mean R' 0.738, R_{yz} 5.37 and T_{yz} 3.276 (Table 1).

3.5. Sheath folds within ignimbrites

Sheath folds developed within ignimbrites have only recently been recognised by Branney et al. (2004) who record metre scale sheath folds and eye structures in several different ignimbrite flows (Fig. 2i,j). They conclude that such curvilinear folds are common within intensely rheomorphic ignimbrites, irrespective of their chemical composition or volcano-tectonic setting. Sheath folds formed in ignimbrites typically display elliptical ratios between 3 and 7 (mean 4.87), with few eyes exhibiting ratios >8 (Fig. 4i, Table 1). Overall, our analysis of data presented in Branney et al. (2004) records consistent (100%) cats-eye patterns (Figs. 4i, 5a) associated with a well-defined trend on eye-charts.

The relatively low R' value (R' 0.713) observed in sheath folds developed in ignimbrites indicates a slightly more pronounced difference between inner and outer elliptical ratios compared to most other lithologies (Table 1). This, coupled with the relatively low elliptical ratios (mean 4.87), may suggest only a limited component of subsequent flattening (which would affect the entire sheath fold equally) during compaction and cooling of the ignimbrite. Typical estimates of compaction within pyroclastic deposits are in the order of 45%, with the amount of compaction increasing downwards through deposits (see Quane and Russell, 2005). It should however be noted that much of the compaction in "high-temperature" ignimbrites occurs *during* actual emplacement (Branney and Kokelaar, 1992). Branney et al. (2004) clearly illustrate that sheath folds clearly deform the rheomorphic fabric associated with non-coaxial strain and emplacement of the deposits. Sheath folds within ignimbrites may thus postdate a significant degree of de-gassing and associated compaction and therefore display R_{yz} and T_{yz} ratios broadly similar to other surficial flows.

3.6. Sheath folds within laboratory models

Physical modelling of sheath folds has been undertaken by a number of authors, most notably Cobbold and Quinquis (1980), Mulugeta and Koyi (1987), Brun and Merle (1988), Marques and Cobbold (1995) and Rosas et al. (2002). Sheath folds displaying up to 110° of hinge-line curvature have also been produced during modelling of shear zones by Bons and Urai (1996), and also during modelling of salt diapirs by Jackson and Talbot (1989) and Jackson et al. (1990). It is important to realise that a variety of mechanisms have been used to generate the precursor folds in different models. These include folds generated by: the passive amplification of initial irregularities during simple shear (e.g. Cobbold and Quinquis, 1980); non-cylindrical irregularities at the base of combined pure and simple shear flow (e.g. Brun and Merle, 1988); and flow perturbations around rigid inclusions (e.g. Marques and

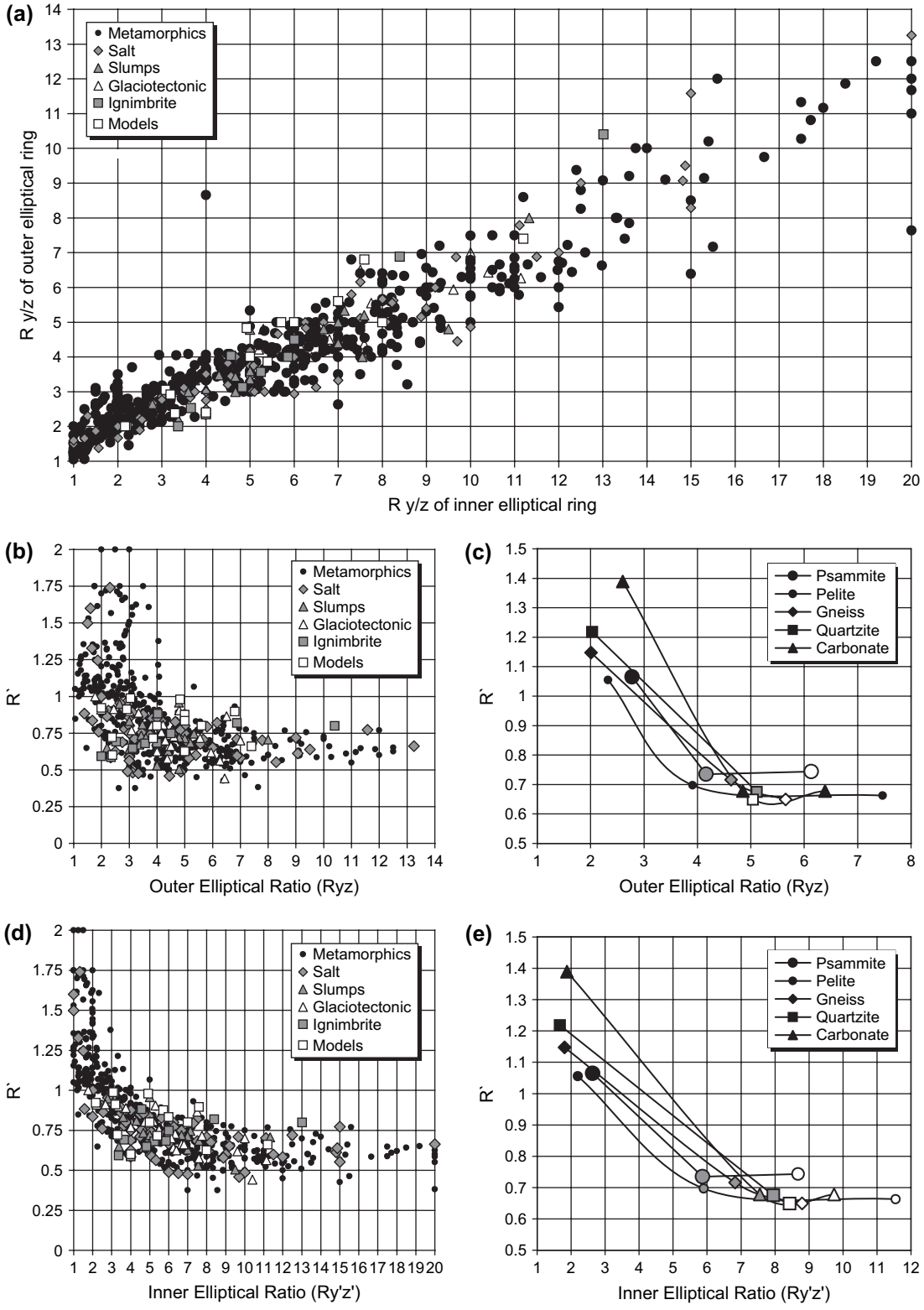

Fig. 5. (a) Eye-chart comparing the outer (R_{yz}) and inner ($R_{y'z'}$) elliptical ratios of individual sheath folds ($N = 620$). Charts comparing (b,c) the outer (R_{yz}) elliptical ratio with R' ($R_{yz}/R_{y'z'}$), and (d,e) the inner ($R_{y'z'}$) elliptical ratio with R'. Plots (c,e) refer exclusively to metamorphic lithologies with mean values for sheath folds developed during constriction shown by solid (black) symbols, simple shear by grey symbols and general shear by open (white) symbols. Bulls-eye-folds ($R' > 1$) are typically developed where inner and outer elliptical ratios are less than 3, whilst cats-eye-folds ($R' < 1$) are largely confined to elliptical ratios >3. Refer to Tables 1 and 2 for detailed values and text for discussion.

Table 2
General patterns of metamorphic sheath folds developed in varying lithologies during different deformation conditions

	Carbonate	Quartzite	Psammite	Gneiss
Simple shear (N = 345)				
N	57	55	160	110
Mean *R*	6.156	6.067	4.8	5.305
R_{yz} (outer)	4.853	5.114	4.162	4.63
$R_{y'z'}$ (inner)	7.553	7.953	5.866	6.825
R'	0.678	0.675	0.735	0.716
Mean T_{yz}	3.182	3.061	3.405	3.370
General shear (N = 353)				
N	41	116	165	23
Mean *R*	8.135	6.419	6.998	7.4996
R_{yz} (outer)	6.391	5.0412	6.131	5.653
$R_{y'z'}$ (inner)	9.734	8.434	8.678	8.792
R'	0.678	0.6484	0.744	0.6494
Mean T_{yz}	5.065	4.034	4.4002	4.318
Constriction (N = 333)				
N	125	33	82	73
Mean *R*	2.154	1.937	2.763	1.953
R_{yz} (outer)	2.602	2.029	2.777	2.008
$R_{y'z'}$ (inner)	1.878	1.673	2.635	1.805
R'	1.389	1.218	1.065	1.1474
Mean T_{yz}	3.170	2.632	3.131	2.422

Cobbold, 1995; Rosas et al., 2002). Marques and Cobbold (1995) claim that the shape of the rigid experimental inclusion partially controls the shape of the resulting sheath fold. Sheath folds formed in laboratory models typically display elliptical ratios between 2 and 8, with few sheaths developing ratios >12 (Fig. 4k, Table 1). All of the experimental sheaths we have analysed display cats-eye-fold patterns (Figs. 4l, 5a) with R' 0.816 and T_{yz} 3.23 (Table 1).

3.7. Sheath folds within pseudotachylytes

Sheath folds have been recorded on the sub-millimetre scale within flow patterns associated with injection of pseudotachylyte veins (e.g. Berlenbach and Roering, 1992; Theunissen et al., 2002; Rowe et al., 2005). Such sheath folds are typically bisected by the flow lineation within the pseudotachylyte. Flow rates in the centre of pseudotachylyte injections have been estimated to be in the order of 10 mm $s^{-}1$ by Bjørnerud and Magloughlin (2004). The geometry of the sheath folds are controlled by viscous drag forces generated within the injected melt, with irregularities in the vein walls further encouraging sheaths to develop. Data from sheath folds within pseudotachylyte is limited ($N = 10$), but they display predominantly bulls-eye patterns (R' 1.162) with low elliptical ratios (R_{yz} 2.99, $R_{y'z'}$ 2.66) suggesting a component of constrictional deformation as flow converges around irregularities.

3.8. Sheath folds within ice

Flow in ice sheets has been modelled by Jacobson and Waddington (2004) in terms of general shear with varying components of pure shear with vertical shortening and bed-parallel simple shear. They suggest that in such regimes, open upright precursor folds may rapidly amplify into recumbent folds with overturned limbs. Indeed, recumbent sheath folds in ice have been reported by Hudleston (1992) who describes macroscopic eye shaped closures measuring hundreds of metres and defining typical (R_{yz} 5.8) elliptical ratios (Fig. 5a). Goodsell et al. (2002) also record metre scale sheath folds within glacial ice displaying cats-eye-fold patterns with overall mean values of R' 0.830, R_{yz} 4.89, $R_{y'z'}$ 5.87 and T_{yz} 4.26.

3.9. Results

Sheath folds generated within surficial flows (sediment slumps, glaciotectonites, ignimbrites, ice) typically display $R' < 1$ cats-eye-folds, with sheaths generated in salt also displaying $R' > 1$ bulls-eye-folding in some cases (Fig. 5a–c). General elliptical ratios are the same across sheath folds developed in metamorphic rocks and surficial flows, with similar R' 0.7 values when elliptical ratios >6 (Fig. 5b,d). R' values are seen to progressively increase as elliptical ratios systematically decrease for values <6, culminating in $R' > 1$ bulls-eye-folds (Fig. 5b,d). In detail, sheath folds developed in different metamorphic lithologies display slightly different elliptical ratios and R' values (Fig. 5c,e). Sheath folds generated under constrictional deformation regimes plot in a distinct $R' > 1$ field with those developed in carbonate and quartzite displaying the most extreme R' values (Fig. 5c,e). Sheaths formed in simple and general shear display similar cats-eye-folds ($R' < 1$), although those formed in general shear are marked by more pronounced elliptical ratios especially in carbonate and pelite (Fig. 5c,e).

Thus, our analytical results (Figs. 4, 5) show that despite the diverse nature of the materials and systems involved, similar y–z elliptical ratios are recorded from sheaths folds in each of these different settings. Sheaths typically show elliptical ratios R_{yz} in the 4.0–4.3 range, whilst inner elliptical ratios are more pronounced typically displaying $R_{y'z'}$ 5.9–6.3 in natural examples (Figs. 4, 5, Table 1). Sheath folds developed within surficial flows (sediment, ignimbrites, etc.) are dominated by simple shear deformation, coupled with an additional (minor?) component of gravity-induced pure shear with vertical shortening resulting in overall general shear. This is reflected in the typical cats-eye ($R' < 1$) fold patterns of associated sheath folds which most closely resemble sheaths generated during broadly simple shear deformation in metamorphic psammites and gneisses (Tables 1, 2). Clearly each of the materials and settings investigated from metamorphic shear zones to surficial flows will have very different viscosities and strain rates that may influence the ultimate geometry of the resulting structure and which are now discussed further.

4. Does sheath fold geometry vary with strain rate?

Strain rates associated with sheath folding are likely to display considerable variation, both *within* each of the settings and obviously *between* different settings. Typical values for crustal flow associated with shear zones are in the range of 10^{-15}–10^{-13} s^{-1}, whilst salt flows display rates typically in the range of 10^{-8} s^{-1}

(e.g. Weijermars, 1997, p. 134). Sedimentary slumps and ignimbrites are considerably more rapid (10^2–10^4 s^{-1}) (Table 1). Similar large variations are recorded in the typical viscosities of these deforming materials, with 10^{20}–10^{24} Pa S estimated for metamorphic rocks, and 10^{16}–10^{18} Pa S for salt whose properties vary dramatically with the addition of water. Van der Wateren et al. (2000) note that strain rates in saturated sediment beneath temperate glaciers are 10^{-7} s^{-1}. This is several orders of magnitude faster than the strain rates developed typically in metamorphic shear zones, with Van der Wateren et al. (2000, p. 268) also noting that such high simple shear strain rates result in the pure shear component (vertical shortening due to loading of ice) forming a relatively small component of total deformation. Therefore, despite the loading effect, sheaths developed in sub-glacial sediments display similar elliptical ratios (R' 0.738, R_{yz} 4.47) to other surficial flows (Table 1).

Thus, in spite of widely varying strain rates (and viscosities) in different settings, elliptical y–z sections display similar mean ratios in metamorphics (R_{yz} 4.2), salt (R_{yz} 4.3), soft-sediment deformation and slumps (R_{yz} 4.3), glaciotectonised sediment (R_{yz} 4.5), and ignimbrites (R_{yz} 4.3) with an overall mean elliptical ratio of R_{yz} ~4.3 (Table 1). The variation in strain rate and viscosity characterising each of these systems does not therefore appear to significantly influence the geometry of the resulting sheath folds that display rather uniform R_{yz}.

5. Does sheath fold geometry vary with scale?

Previous work concerning eye-folds in metamorphic rocks has largely concentrated on sheaths developed on less than a 10 m scale (Alsop and Holdsworth, 2006). The present contribution represents the first study to directly compare sheath fold geometries across a wide range of scales, varying from sub-millimetre, to those on a kilometre scale as reported by Alsop (1994), Seno et al. (1998) and Ganesan et al. (1999), to recumbent sheath ''nappes'' as proposed by Vollmer (1988), Liu et al. (1997), Orozco et al. (2004), Searle and Alsop (2007). Although it has been recognised that sheath folds may develop at these very different scales, this analysis allows us to determine for the first time whether sheaths display self-similar patterns, or show characteristic changes in geometry which vary as a function of scale (self-affine).

5.1. Multi-scale sheath folds

In order to address the points noted above, paired measurements of y and z axes from individual sheath folds have been recorded across a range of scales in metamorphic rocks, salt, soft sediment slumps, glaciotectonites, ignimbrites and models (Fig. 6 and summarised in Table 1). Standard graphs of sheath y–z axes in these materials were plotted across a variety of scales. Results were found to be consistent with sheath folds in metamorphic rocks displaying an overall 0.99 R^2 correlation across 9 orders of magnitude (Figs. 6a, 6b, 7a), salt sheaths display 0.96 R^2 correlation (Figs. 6c, 6d, 7a), sheaths in soft sediment slumps display >0.99 R^2 correlation (Figs. 6e, 6f, 7a), sheaths in glaciotectonised sediments also display 0.96 R^2 correlation (Figs. 6g, 6h, 7a), sheaths in ignimbrites display >0.98 R^2 correlation (Figs. 6i, 6j, 7a), and modelled sheaths display 0.94 R^2 correlation (Figs. 6k, 6l, 7a, Table 1). Owing to the range of observed scales which varies from <mm to >75 km (particularly in metamorphics and salt), data is most readily presented on log-log graphs of sheath y and z axes, which plot along a remarkably similar trend through several orders of magnitude (Fig. 7a).

In order to further investigate the similarity in elliptical ratios across a range of scales, mean R_{yz} and R' values were plotted across eight orders of magnitude in metamorphic sheath folds (Fig. 7b,c). R_{yz} values in both bulls-eye and cats-eye folds display broadly similar and consistent values on the millimetre to kilometre scale (Fig. 7b). Sheath folds developed in simple shear and general shear also display characteristic R' values as do those folds generated during constriction (Fig. 7c). The broadly similar values across eight orders of magnitude from outcrop scale (where all structural relationships may be clearly observed) to >km scale suggests that analysis and interpretation are not unduly affected by sampling issues (see Section 6.5). The role of scale in folding has been summarised by Ramsay and Huber (1987, p. 206) who suggest that gravity plays only a minor role in folds with wavelengths of <100 m, whilst folds with wavelengths of >30 km cannot be formed by compression alone and require the operation of gravity to some extent. Within the present study, no analysed sheath folds display z axes of more than 20 km. Thus, sheath geometries do not vary markedly with scale (Fig. 7), with the typical straight-line relationships seen on R_{yz} and R' graphs and log-log plots indicating that ratios associated with larger structures are not being unduly influenced by gravitational forces (or sampling bias).

5.2. Scaling patterns of sheath folds

Short (z) axes of sheath folds in metamorphic shear zones display a range of scales from sub-mm to more than 20 km in one extreme case, although more typically the maximum value varies from the centimetre scale to <8 km. Ninety-five percent of sheath folds in metamorphic shear zones display z axes of <1.6 km. Similarly 95% of sheath folds in salt flows and diapirs display z axes of <400 m. Sheath folds observed in glaciotectonised sediments, soft-sediment slumps, and ignimbrite flows are marked by being of relatively small scale, with 90% of z axes <2 m, 1 m and 1 m, respectively. Data were plotted on log cumulative frequency plots and show a central straight segment extending over 4 orders of magnitude (from ~1 mm to 100 m) (Fig. 6). This suggests similar controls on sheath development at this range of scales. Grain scale processes may predominate within sheath folds developed below the millimetre scale, whilst direct observations of sheath folds greater than 100 m are hampered by a typical lack of continuous outcrop. It is notable that fewer sheath folds are recorded and analysed with y axes on the 10 m to 1 km scale in metamorphic shear zones. Sheath folds analysed via aerial photography in salt are however common at this scale suggesting that the pattern may reflect the problems of sampling features which are typically too large for outcrop studies and too small for regional maps (see also Hippertt, 1999).

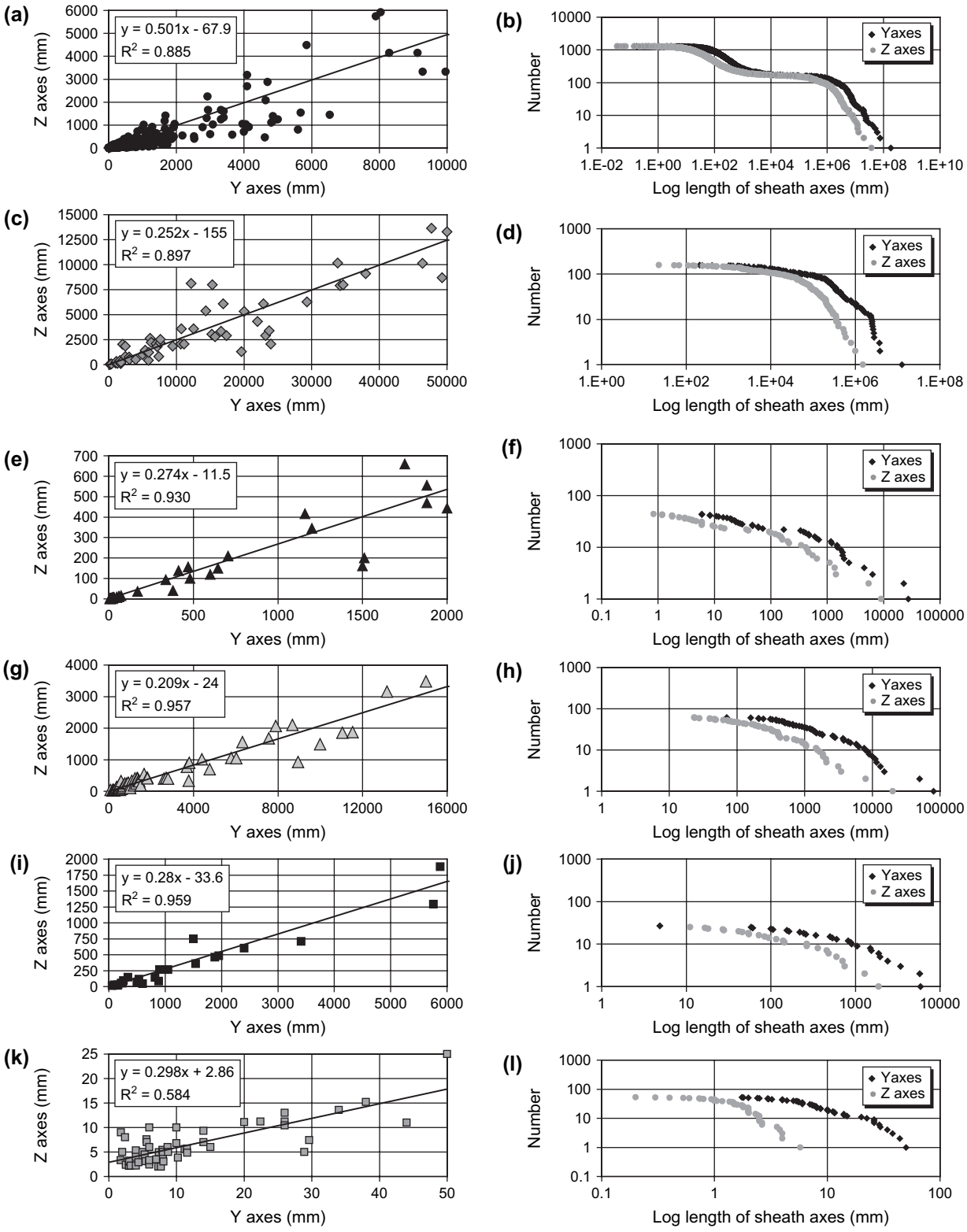

Fig. 6. Plots of y and z lengths of sheath fold axes (mm) and log cumulative number versus log y and z axes for sheath folds developed in (a,b) metamorphics (sheaths with y axes between 0 and 10 m) ($N = 1103$), (c,d) salt (sheaths with y axes between 0 and 50 m) ($N = 55$), (e,f) soft sediment slumps ($N = 47$), (g,h) glaciotectonic sediments ($N = 59$), (i,j) ignimbrites ($N = 25$), (k,l) models ($N = 53$). Reduced major axis regression trend lines and R^2 values are also given. The central portion of the data in the log cumulative number plots which defines a straight line relationship is typically considered to reflect the scale at which data are defining close to self-similar characteristics and similar structural controls are operating.

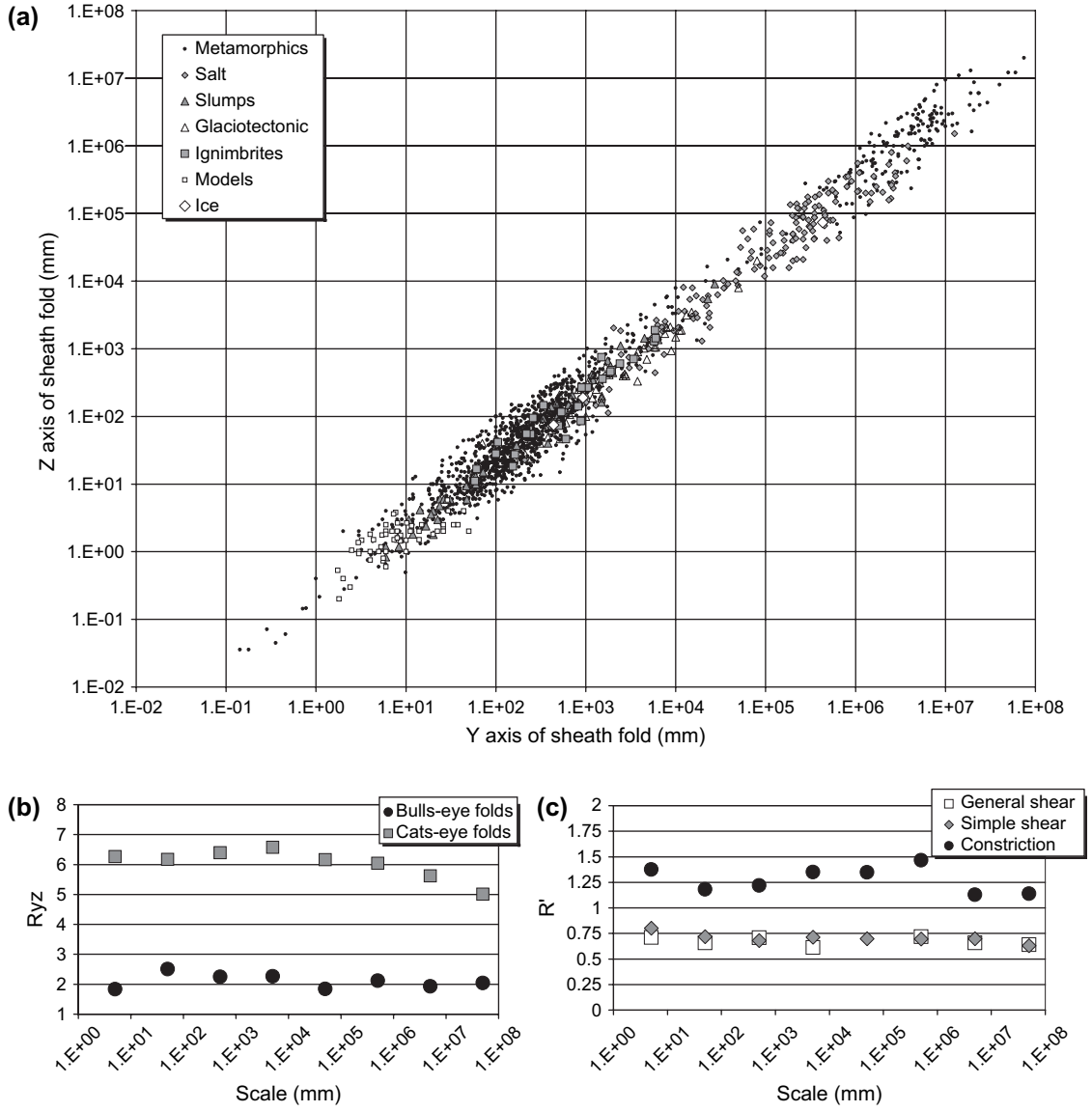

Fig. 7. Logarithmic plots of the intermediate (y) and short (z) axes of sheath folds displaying a range of scales and materials. (a) Combined log-log plot of all data set illustrating the remarkably similar range of elliptical (y–z) ratios in sheath folds from a variety of materials and range of scales (y axes vary from <0.1 mm to >75 km). See text for further discussion. (b,c) Plots illustrate (mean) R_{yz} and R' across a range of scales (1 mm to 100 km) to define cats-eye and bulls-eye-fold patterns generated during simple shear, general shear and constrictional deformation. The broadly similar values across eight orders of magnitude from outcrop scale (where all structural relationships may be clearly observed) to >km scale suggests that large scale structures are not being misidentified. See text for further discussion.

Thus, the majority of sheath folds in metamorphic rocks are observed on a metre scale, with <10% of sheaths displaying y axes of more than 1 km. Whilst this skewing of the data towards smaller scales may reflect the ease of interpretation of outcrop scale structures noted above, it may also mirror the scale of most natural high strain zones in which sheath folds are generated.

5.3. Scale of sheath folds and shear zones

Simple geometric models of mildly curvilinear folds developed at high angles to moderate non-coaxial deformation clearly demonstrate that the short (z) axis of the resulting sheath fold cannot be greater than the thickness of the deformation zone itself (e.g. Ramsay, 1980; Lacassin and Mattauer, 1985; Skjernaa, 1989; Mies, 1993) (Fig. 8). Kilometre scale sheath folds may also display marked variations in the degree of minor fold and fabric rotation from the upper to lower limbs of the major fold (see Alsop and Holdsworth, 2004b). Such systematic patterns of deformation about the major structure are clearly *inconsistent* with models of rolling hinges or narrow, high-strain zones sequentially migrating across existing structures. However, progressive variation in the intensity of non-coaxial deformation from the upper to lower limbs of major folds is consistent with a broad zone of heterogeneous shear affecting the *entire* sheath fold. The relatively small scale sheath folds observed in surficial flows and glaciotectonised sediments, where z axes are typically 1–2 m, simply reflects the limited thickness of the deforming

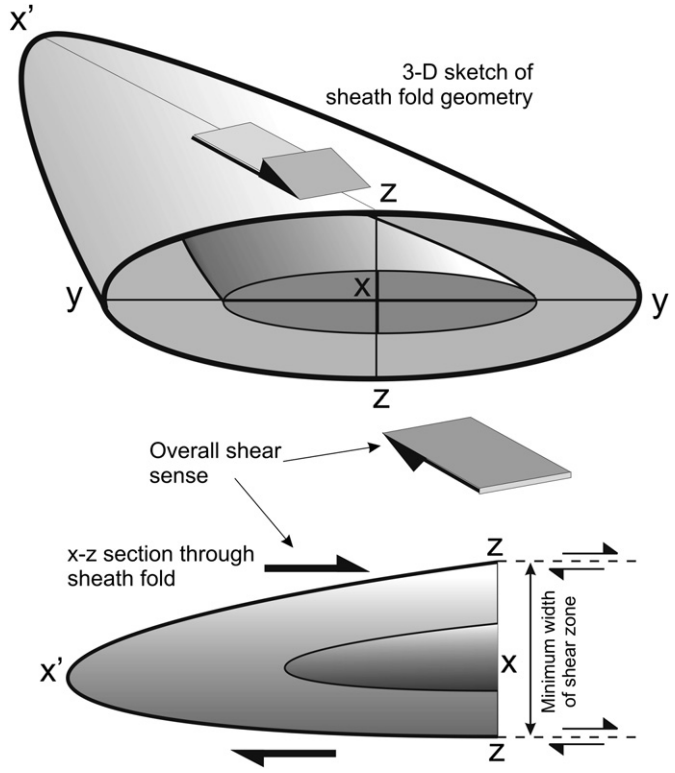

Fig. 8. Schematic 3-D sketch (above) and x–z section (below) illustrating the relationship between the widths of high strain zones and the constraints they impose on the dimensions of sheath folds (see text for discussion).

unit. This suggests that individual sheaths form synchronously rather than via a narrow deformation zone migrating sequentially through the fold. Indeed, Van der Wateren et al. (2000) recognised that metre scale sheath folds developed during sub-glacial shearing of sediments reflected the thickness of the deforming zone. Thus, rather than a relatively thin high-strain zone migrating sequentially through a sub-glacial sequence (see Boulton, 1996), the sheath folds suggest shearing may actually take place over several metres to generate these coherent structures. The *maximum* (z) axis measured in elliptical (y–z) sections through the body of a sheath fold will thereby provide a *minimum* constraint on the thickness of the deformation zone (Fig. 8). Sheath folds will not develop if the scale of the precursor fold is significantly larger than the width of the deformation zone itself. This fundamental scaling relationship suggests that many precursor folds which subsequently develop into sheath folds actually form early during the same progressive deformation event that generates the sheaths. Thus, the size of sheath folds may not only reflect the thickness and continuity of marker layers that define the folds, but also the scale of strain localisation and shearing processes.

In summary, characteristic R' and R_{yz} ratios developed across a range of scales suggest that: (a) the processes responsible for the development of sheath folds also operate across 9 orders of magnitude; (b) that the major controls on sheath fold geometry do not vary significantly over this range of scales; (c) the scale of sheath folds provides minimum constraints on the width of shear zones active at any one time.

6. Discussion on the role of precursor folds, deformation, lithology and scale on sheath folding

The final elliptical ratio (R_{yz}) and R' value of any sheath fold may in part reflect a number of variables. The overall similarity of R_{yz} ratios across the range of studied environments and scales noted above suggests that the same controls on sheath fold geometries have operated in these very different materials and settings. These controls may include (a) the geometry of precursor folds, (b) the type and magnitude of deformation, (c) the type of lithology, and (d) the scale of deformation. The large variation in estimated strain rate and viscosity between settings when compared to the similarity of sheath fold geometries suggests that these factors have only a relatively limited effect.

6.1. The role of precursor fold geometry in sheath fold development and analysis

In this study we are particularly concerned with the variation in inner ($R_{y'z'}$) and outer (R_{yz}) elliptical ratios (R') which typically define cats-eye fold patterns ($R' < 1$) through sheath folds. The more pronounced inner elliptical ratios observed in cats-eye folds may be a consequence of several factors and controls discussed below.

6.1.1. The 3-D geometry of precursor folds

The geometry and orientation of the precursor fold will clearly influence the shape of the resulting sheath which evolves during subsequent shearing (e.g. Skjernaa, 1989; Mies, 1993; see Alsop and Holdsworth, 2006 for details). Folds displaying rounded outer arcs and tightly pinched inner arcs have been recorded within high strain zones across a range of environments including salt (e.g. Talbot and Koyi, 1998). The cross sectional morphology of these folds (including sheath folds), is considered typical of buckling folds (e.g. Ghosh, 1993, p. 524) which have undergone subsequent fold modification during high strain (e.g. Platt and Lister, 1985). As many folds developed in shear zones initiate via a buckling mechanism, the rounded outer-arcs and pinched inner-arcs of individual precursor fold surfaces may naturally create an inherent cats-eye fold pattern in many subsequent sheaths. In addition, the outer-most layer which is obviously the largest fold (and may also be the thickest layer if initiated by buckling) may help control the inner folds, i.e. the inner-arc geometry of the outer layer dominates adjacent smaller scale folds. However, whilst the outer-most ellipse (R_{yz}) will correspond typically to an outer-arc fold, the inner ellipse may not *necessarily* coincide with a ''pinched'' inner arc surface, i.e. a nested sheath fold will incorporate several layers each with its own inner and outer arcs. Alternative mechanisms of generating cats-eye fold patterns therefore require consideration and are discussed below.

6.1.2. The 3-D geometry of individual sheath surfaces

Minnigh (1979) and Crispini and Capponi (1997) have undertaken detailed y–z serial sectioning along the length (x) of

individual sheath folds. Analysis of these sections reveals that the $y-z$ elliptical ratio for any individual surface may increase towards the nose or apex of that particular sheath. A single cross section (or erosion surface) through the sheath fold will thus intersect the surface defining the inner-most sheath closer to its nose, and hence display greater R_{yz} values associated with overall cats-eye ($R' < 1$) patterns. R_{yz} values may increase towards the nose of cats-eye folds as reductions in the length of the short (z) axis related to inter-limb angles have a proportionally greater effect on this ratio than reductions in y controlled by the apical angle.

These geometries may reflect the original shape of the precursor fold as most periclinal folds display pronounced changes in fold hinge geometry along the length of the curvilinear hinge (Dubey and Cobbold, 1977; Price and Cosgrove, 1990, p. 263). Sections through the central portion (culminations/depressions) of periclines display more angular profiles associated with tighter inter-limb angles when compared to sections near terminations at each end of the fold. When subjected to subsequent shearing, the central portions of the folded surface will therefore display the greatest $y-z$ ratios, which will progressively diminish towards each end of the fold. As a single section through any ''nested'' set of sheaths will cut closer to the nose of the inner-most sheath, then the characteristic cats-eye ($R' < 1$) patterns noted above will typically result.

6.1.3. The 3-D geometry of sheath fold packages

Sheaths may also develop more intense inner R_{yz} values due to variations in the original shape of multi-layer folds along their axial surface. Most folds will display amplitudes which progressively decrease and die out when traced along their axial surface, i.e. greatest amplitudes are in the centre of the fold package. If this package is then sheared then the central portion (which originally was marked by tighter folds with more pronounced hinge curvilinearity) will display the greater R_{yz} values. Lesser R_{yz} values will occur on either side of this central package. Because of the enhanced curvilinearity of ''central'' folds during shearing, we observe intense folds within less intense folds. We are unlikely to see lower R_{yz} within higher R_{yz} as (a) gentle folds do not grow as much in amplitude/curvilinearity during subsequent shearing, and (b) the fold package may lie on a decollement so we only see intense folds progressively diminishing ''upwards'' along their axial surface.

Thus, the geometry of precursor buckle folds, coupled with internal ''stacking'' or ''nesting'' of sheaths one within the other collectively explain why inner-most sheath ratios ($R_{y'z'}$) differ consistently from the outer-most R_{yz}. As sheath fold $y-z$ ratios are shown to vary systematically along the length (x) of any sheath it also follows that single cross sections will provide cuts at different relative positions through adjacent sheath surfaces. These concepts reflecting the nucleation and enhanced development of the core of the precursor fold were briefly noted by Alsop and Holdsworth (2006, p. 1601) and provide a geometric mechanism to explain the R' variations observed in cats-eye fold patterns.

6.2. The role of deformation in sheath fold development

From an analysis of sheath folds formed within metamorphic rocks, Alsop and Holdsworth (2006) have demonstrated that elliptical ratios (R_{yz}), R' and variations in layer thickness (T_{yz}) vary systematically around sheath folds and directly reflect the type of simple shear, general shear or constrictional deformation associated with sheath fold development. Although conditions for constrictional flow may be created locally in surficial flows via the narrowing of confining valleys and channels, such situations appear to be relatively uncommon. Significantly, no bulls-eye patterns are found associated with gravity-driven non-coaxial deformation within soft-sediment slumps, glaciotectonised sediments or ignimbrite flows. The vast majority (>90%) of sheath folds developed in surficial flows (salt, sedimentary slumps, ignimbrites, ice) display cats-eye-fold patterns ($R' < 1$) and are considered to reflect gravity-driven deformation associated with simple/general shear. Analysis of sheath folds developed within salt diapirs reveals a minor component (10%) of bulls-eye-fold patterns considered to reflect constrictional deformation. Such constriction may be produced by the convergent flow of salt from a source layer into a diapiric neck, e.g. Upheaval Dome (Jackson et al., 1998); Pugwash Diapir (Carter, 1990a,b,c; Alsop et al., 2000).

In summary, sheath folds from salt diapirs and metamorphic shear zones display almost identical, well-defined ($R^2 > 0.9$) outer to inner elliptical ratios and patterns as do soft-sediment slumps and glaciotectonised sediments reflecting cats-eye-folds. Data collected across the range of settings and materials from metamorphic shear zones to surficial flows are therefore consistent with simple shear and general shear dominated deformation being a major factor in the development of sheath fold geometries. Whilst bulls-eye-folds associated with constrictional deformation may be well-developed within some metamorphic shear zones and locally within salt diapirs, their overall scarcity in surficial flows suggests that the effects of constriction are typically limited.

6.3. The role of lithology in sheath fold development

It has long been recognised that mechanical and rheological effects associated with lithological variation play a dominant role during the initial stages of fold development during simple shear, whereas later amplification and rotation of folds is largely governed by kinematics (e.g. Berthe and Brun, 1980). Field observations of fold styles (Holdsworth, 1989, 1990; Alsop and Holdsworth, 2007) and physical modelling of shear zones by Bons and Urai (1996) have also shown that sheath folds typically initiate by buckling of layers rather than passive amplification of initial perturbations as suggested by Quinquis et al. (1978). The mechanical controls on such buckling are considered to be heterogeneities within the folded layer itself coupled with interaction with adjacent layers and folds. The occurrence of boudinaged layers within some sheath fold complexes also indicates that layering has not been entirely passive (e.g. Merschat et al., 2005).

The greater R' values recorded in sheath folds in salt and surficial flows (Table 1) when compared to metamorphic examples generated during simple and general shear (R' 0.69) indicates less variability between inner and outer elliptical ratios. This may suggest less rheological contrast and associated buckling between adjacent layers in sheath folds developed in salt and surface flows. Variability in R' values also occurs between different types of metamorphic rocks with sheath folds developed in quartzite and carbonate displaying the lowest R' value during simple/general shear, whilst sheaths in psammite display the greatest R' (Table 2). Conversely, during constrictional deformation, sheath folds developed in quartzite and carbonate display the greatest R' values whilst those in psammite are marked by lower R' values (Table 2). The relatively high R' value (R' 0.816) within laboratory models of sheath folds compared to natural systems may also reflect less rheological contrast between modelled layering.

Thus, the observations noted above support curvilinear fold initiation by buckling, triggered by inhomogeneous deformation or mechanical heterogeneity within the deforming material. Curvilinear buckles and periclines acting as precursor folds to sheaths may help explain the tighter inner fold geometries which are then further modified and accentuated during subsequent shearing to create the cats-eye fold geometries. The typically greater R' values recorded in sheath folds from salt and surficial flows may suggest less rheological contrast between layers when compared to those observed in metamorphic rocks.

6.4. The role of scale in sheath fold development

The presence of large scale sheath folds which display coherent geometries suggests that deformation partitioning may not be significant on the scale of the sheath. Large scale sheath folds may however be composed of several smaller folds which largely reflects the scaling patterns of the precursor folds. Such second order sheath folds may display asymmetric hinge-lines which define patterns of fold hinge-line vergence towards the larger scale sheath closure (Alsop and Holdsworth, 1999). Miller et al. (2002) record intense non-coaxial shear and note that whilst extreme fold axis variability may be recorded in thinner bedded units, more massive units display cylindrical hinges at high angles to the mineral lineation. Similarly, Salinas-Prieto et al. (2000) illustrate complex minor curvilinear folds which anastomose with one another during overall simple shear deformation. It is considered that the geometry of small scale sheath folds may vary with local changes in strain magnitude and type from the upper to lower limbs of major fold nappes that may themselves display curvilinear hinge geometries. Sheath folds are resilient to subsequent deformation and as such may provide a more reliable record of deformation than grain fabrics that may be readily overprinted and destroyed. An example of this is provided by Beunk and Page (2001) who measure prolate clasts in deformed metaconglomerates and suggest constrictional deformation at this scale. However regional mapping of large scale sheath folds by Beunk and Page (2001) reveals kilometre scale eye patterns with y axes extending for up to 15 km. These sheaths define overall cats-eye-fold patterns (R' 0.74) with calculated R_{yz} 3.74. Differences in strain recorded by large scale sheath folds and pebbles may reflect discrepancies between the clast and matrix viscosities, together with local partitioning of strain types and finite strain histories of clasts.

The short (z) axis of the sheath fold is controlled by (a) the size of the precursor fold and (b) the width of the active deformation zone. The z axis thus provides a minimum thickness for the zone of active shearing at any given time, whilst the intermediate y axis provides the minimum width of the deforming flow cell thereby constraining the minimum dimensions of the zone of active deformation. Classical buckling theories (Biot, 1957; Ramberg, 1963) using linear elastic and viscous mechanics suggest that folding initiates only when mechanical contrasts between layers is >100 producing a dominant wavelength which amplifies to give periodic fold systems (Hobbs et al., 2000, 2007). It is difficult to envisage how periodic precursor folds would amplify to produce scale-invariant sheath forms over 9 orders of magnitude scale range. Recently, Hobbs et al. (2007) show that for a coupled thermal-mechanical system, folds may form at many length scales in systems with low viscosity contrasts. We suggest here that amplification of precursor folds with a range of length scales would be the most appropriate way to initiate the scale-invariant sheath folds we observe. In the coupled thermal-mechanical system modelled by Hobbs et al. (2007), temperature effects from mechanical dissipation in turn affects the strength of temperature-dependant rheologies typical of the mid-lower crust and would be appropriate for the metamorphic, salt and ignimbrite sheath folds we observe. Analogous coupled systems whereby fluid is coupled to effective stress could produce similar effects for soft sediment and glaciotectonic sheath folds. Thus, the scale of sheath folds reflects the mechanical properties of the deforming material coupled with the scale of shear zones to generate sheaths in addition to the scale and continuity of lithological banding that define the sheaths. Large scale sheath folds with z axes extending for up to 20 km may thus ultimately provide information on 3-D crustal deformation patterns associated with large scale crustal deformation regimes such as channel flow (e.g. Merschat et al., 2005; McCaffrey et al., 2006).

6.5. Scaling and sampling issues in sheath fold analysis

As with any structural analysis across a range of scales, a number of issues concerning sampling and scaling patterns of sheath folds may be identified. As the recognition of sections through sheath folds involves the identification of oval or eye-shaped patterns, it may be suggested that it may be easier to ''spot'' or sample sheaths with lower y–z ratios (e.g. Williams and Zwart, 1977; see also Alsop and Holdsworth, 2006). It is interesting to note therefore that in all environments, sheaths with $R_{yz}<4$ actually form the minority of the measured data, and that all data sets do include sheaths with $R_{yz}>10$.The presence ($\sim$10%) of sheaths displaying $R_{yz}>10$ across a range of scales (and therefore different ''sampling'' procedures) from outcrop ($<$10 m) to aerial photo/map ($>$1 km) and across both metamorphics and salt (the two datasets which span this range) provides

further reassurance over sampling procedures. The observation that metamorphic sheaths generated during general shear (in which a flattening component typically increases R_{yz} during shear) incorporate many more ($\times 3.5$) $R_{yz} > 10$ when compared to simple shear formed sheaths lends further support to the overall validity of the dataset.

Clearly the elliptical ratios and identification of the outer-most rings of sheath folds is to some extent dependent on, and reflects the constraints imposed by, the scale of observation. In outcrop (and smaller) sheath folds, the outer-most ellipse is typically bounded by layers displaying double vergence fold geometries, and as such the observer can be sure of the extent of R_{yz}. Similarly, the inner-most ellipse ($R_{y'z'}$) is obviously bounded by this outer layer and the R' value may thus be calculated. Large scale (y axes >1 km) closure patterns are normally defined by aerial photographs and/or mapping which also typically permits the outer-most ellipse to be identified. As elliptical ''rings'' within sheath folds define progressive variations in R_{yz} from the outer-most to the inner-most ellipses, then the misidentification of the outer-most ellipse will result in overall R' values closer to 1 in both cats-eye and bulls-eye folds (i.e. differences between the inner- and outer-most ellipses will be less pronounced as the outer-most ellipse representing the most extreme y–z has not been measured). If one had systematically misidentified the outer-most ellipse in larger scale sheaths then this should be reflected in mean R' and R_{yz} values across the range of scales. Our analysis of the data (Fig. 7b,c) shows that mean R' and R_{yz} are in fact relatively constant across all orders of magnitude in both cats-eye and bulls-eye fold packages, suggesting that measurement/interpretative error has not significantly influenced our results.

7. Summary

Sheath folds display broadly similar inner- and outer-most elliptical y–z ratios across a wide variety of materials and environments. These observations suggest fundamental geometric and mechanical constraints on the initiation and evolution of sheath folds that apply across several orders of magnitude and strain rate. The scale invariant nature of sheath folding may reflect the thickness of the deformation zone. The wavelength of fold hinge-line curvilinearity is typically greater for larger folds of thicker units, with curvilinear folds generated on a single surface typically displaying similar hinge-line wavelengths (e.g. Ghosh and Sengupta, 1984). Analysis of lineation patterns around curvilinear folds by Ghosh and Sengupta (1984) indicates that passive amplification of buckle folds into highly curvilinear (sheath) folds occurs after the buckle folds themselves have already become very tight with an associated increase in hinge curvature. Experimental studies also suggest more pronounced non-cylindricity is generated in mechanically heterogeneous materials (e.g. Ghosh and Ramberg, 1968; Dubey and Cobbold, 1977). Rhodes and Gayer (1977) note that the degree of curvilinearity displayed by large scale fold hinges may be relatively small ($<10°$), whilst associated minor folds are markedly non-cylindrical with hinges exhibiting $>90°$ of curvature to define sheath fold geometries. In addition, a number of authors have noted the apparent lack of minor sheath folds associated with the development of major sheath structures (e.g. Henderson, 1981; Lacassin and Mattauer, 1985; Fowler and El Kalioubi, 2002). Such observations and inferences question the assumption that minor structures are geometrically akin to larger scale features of similar type.

The recognition in this study of consistent fold patterns developed across several orders of magnitude and within different materials suggests that bulk strain type coupled with this fundamental mechanical behaviour is the governing control on sheath folding. This suggests that models of sheath development by passive shearing may be more appropriate in most cases as we may otherwise expect to observe a greater scale and material dependence associated with mechanical significance of layering. Thus, the layering and banding that defines sheath folds may be rheologically significant during the generation of precursor buckle folds across a broad range of materials and environments. However, with continued deformation, the layering marking the original folds may become increasingly passive to define sheath folds.

8. Conclusions

Sheath folds have been carefully documented by a host of authors from a wide variety of materials in different geological settings. Analysis of this published work, together with our own observations, allows us to make some general remarks and draw some conclusions about sheath fold geometries and deformation. This study suggests that:

(a) A similar range of elliptical y–z ratios (R_{yz}) are recorded in cross sections of sheath folds from metamorphic shear zones (R_{yz} 4.2), salt flows (R_{yz} 4.3), soft-sediment slumps (R_{yz} 4.3), glaciotectonites (R_{yz} 4.5), and ignimbrite flows (R_{yz} 4.3) with an overall mean elliptical ratio $R_{yz} \sim 4.3$. These characteristic R_{yz} values that are developed across a variety of materials suggest that similar processes are responsible for the development of sheath folds across a range of geological environments and strain rates.

(b) Gravity-driven surficial flows are dominated by cats-eye-fold patterns ($R' < 1$). Such patterns are typically associated with simple shear and general shear-dominated deformation, with greater deformation resulting in tightening of the precursor folds. This is consistent with a buckling mechanism of rheologically significant layers. The well-established relationships between layer thickness and fold wavelength/hinge curvilinearity (e.g. Ghosh and Ramberg, 1968; Dubey and Cobbold, 1977) associated with buckle folding may therefore ultimately determine subsequent sheath fold geometries.

(c) Despite the huge variation in strain rate and viscosity from metamorphic shear zones to surficial flows, scale invariant sheath fold geometries are produced. This suggests that strain rate and viscosity do not pose significant controls. More fundamental constraints are imposed by the scale of the initial instability (buckle fold), and/or the width of the deformation zone coupled with the nature of shear- or constriction-dominated deformation.

(d) Characteristic R_{yz} ratios are developed in sheath folds across a range of scales. No systematic variation occurs in R_{yz} with scale. The frequency of small sheath folds associated with larger ones will depend on the original patterns and geometries of precursor folding. These relationships suggest that processes responsible for the development of sheath folds following initial buckle folding are predominantly passive and operate across several orders of magnitude.

(e) As the length of the z axis of sheath folds reflects the *minimum* thickness across which the shearing process operates in non-coaxial deformation, the R_{yz} measurement therefore provides minimum constraints on the widths and thicknesses of shear zones operating in different settings and throughout the crust.

(f) The largest sheath folds are developed in basement gneisses and display z axes in the order of 20 km. This suggests large scale flow of material (>20 km) consistent with models of mid-crustal channel-flow.

Acknowledgements

Fieldwork for this paper was funded by the Welsh Bequest of the University of St. Andrews, the Edinburgh Geological Society and the Carnegie Trust, together with the proceeds of the Lyell Fund of the Geological Society of London. We wish to thank Sudipta Sengupta, James McLelland and two anonymous reviewers for detailed and constructive comments which have improved this paper.

References

Agar, S.M., 1988. Shearing of partially consolidated sediments in a lower trench slope setting, Shimanto Belt, SW Japan. Journal of Structural Geology 10, 21–32.

Allen, J.R., 1982. Developments in Sedimentology. Elsevier, Amsterdam, 661 pp.

Alsop, G.I., 1994. Relationships between distributed and localized shear in the tectonic evolution of a Caledonian fold and thrust zone, northwest Ireland. Geological Magazine 131, 123–136.

Alsop, G.I., Holdsworth, R.E., 1993. The distribution, geometry and kinematic significance of Caledonian buckle folds in the western Moine Nappe, northwestern Scotland. Geological Magazine 130, 353–362.

Alsop, G.I., Holdsworth, R.E., 1999. Vergence and facing patterns in large-scale sheath folds. Journal of Structural Geology 21, 1335–1349.

Alsop, G.I., Holdsworth, R.E., 2002. The geometry and kinematics of flow perturbation folds. Tectonophysics 350, 99–125.

Alsop, G.I., Holdsworth, R.E., 2004a. Shear zone folds: records of flow perturbation or structural inheritance? In: Alsop, G.I., Holdsworth, R.E., McCaffrey, K.J.W., Hand, M. (Eds.), Flow Processes in Faults and Shear Zones. Special Publications, vol. 224. Geological Society, London, pp. 177–199.

Alsop, G.I., Holdsworth, R.E., 2004b. The geometry and topology of natural sheath folds: a new tool for structural analysis. Journal of Structural Geology 26, 1561–1589.

Alsop, G.I., Holdsworth, R.E., 2004c. Shear zones – an introduction and overview. In: Alsop, G.I., Holdsworth, R.E., McCaffrey, K.J.W., Hand, M. (Eds.), Flow Processes in Faults and Shear Zones. Special Publications, vol. 224. Geological Society, London, pp. 1–9.

Alsop, G.I., Holdsworth, R.E., 2005. Discussion on evidence for non-plane strain flattening along the Moine Thrust, Loch Strath nan Aisinnin, North-West Scotland by Strine and Wojtal. Journal of Structural Geology 27, 781–784.

Alsop, G.I., Holdsworth, R.E., 2006. Sheath folds as discriminators of bulk strain type. Journal of Structural Geology 28, 1588–1606.

Alsop, G.I., Holdsworth, R.E., 2007. Flow perturbation folding in shear zones. In: Ries, A.C., Butler, R.W.H., Graham, R.D. (Eds.), Deformation of the Continental Crust: The Legacy of Mike Coward. Special Publications, vol. 272. Geological Society London, pp. 75–101.

Alsop, G.I., Holdsworth, R.E., Strachan, R.A., 1996. Transport-parallel cross folds within a mid-crustal Caledonian thrust stack, northern Scotland. Journal of Structural Geology 18, 783–790.

Alsop, G.I., Brown, J.P., Davison, I., Gibling, M.R., 2000. The geometry of drag zones adjacent to salt diapirs. Journal of the Geological Society, London 157, 1019–1029.

Balk, R., 1949. The structure of the Grand Saline salt dome, Van Zandt County, Texas. American Association of Petroleum Geologists Bulletin 33, 1791–1829.

Balk, R., 1953. Salt structure of Jefferson Island salt dome, Iberia and Vermillion Parishes, Louisiana. American Association of Petroleum Geologists Bulletin 37, 2455–2474.

Banham, P.H., Ranson, C.E., 1965. Structural study of the contorted drift and disturbed chalk at Weybourne, North Norfolk. Geological Magazine 102, 164–174.

Benediktsson, I.O., 2005. The 1890 and 1964 push moraines at Brúarjökull, a surge-type glacier in Iceland: morphology, sediments and structural geology. Cand. Scient. thesis, University of Copenhagen.

Benkhelil, J., Guiraud, M., Paccolat, J., 1998. Decollement structures along the Cote D'Ivoire-Ghana transform margin. In: Mascle, J., Lohmann, G.P., Moullade, M. (Eds.), Proceedings of the Ocean Drilling Program. Scientific Results, vol. 159, pp. 25–33.

Bennett, M.R., Huddart, D., McCormick, T., 2000. An integrated approach to the study of glaciolacustrine landforms and sediments: a case study from Hagavatn, Iceland. Quaternary Science Reviews 19, 633–665.

Berlenbach, J.W., Roering, C., 1992. Sheath-fold-like structures in pseudotachytytes. Journal of Structural Geology 14, 847–856.

Berthe, D., Brun, J.P., 1980. Evolution of folds during progressive shear in the South American Shear Zone, France. Journal of Structural Geology 2, 127–133.

Beunk, F.F., Page, L.M., 2001. Structural evolution of the accretional continental margin of the Paleoproterozoic Svecofennian orogen in southern Sweden. Tectonophysics 339, 67–92.

Biot, M.A., 1957. Folding instability of a layered viscoelastic medium under compression. Proceedings of the Royal Society, London, A 242, 111–454.

Bjørnerud, M., Magloughlin, J.F., 2004. Pressure-related feedback processes in the generation of pseudotachylytes. Journal of Structural Geology 26, 2317–2323.

Blatt, H., Middleton, G., Murray, R., 1980. Origin of Sedimentary Rocks. Prentice-Hall.

Bons, P.D., Urai, J.L., 1996. An apparatus to experimentally model the dynamics of ductile shear zones. Tectonophysics 256, 145–164.

Boulton, G.S., 1996. The origin of till sequences by subglacial sediment deformation beneath mid-latitude ice sheets. Annals of Glaciology 22, 75–84.

Bradley, D., Hanson, L., 1998. Paleoslope analysis of slump folds in the Devonian flysch of Maine. Journal of Geology 106, 305–318.

Branney, M.J., Kokelaar, P., 1992. A reappraisal of ignimbrite emplacement: progressive aggradation and changes from particulate to non-particulate flow during emplacement of high-grade ignimbrite. Bulletin of Volcanology 54, 504–520.

Branney, M.J., Barry, T.L., Godchaux, M., 2004. Sheathfolds in rheomorphic ignimbrites. Bulletin of Volcanology 66, 485–491.

Brun, J.P., Merle, O., 1988. Experiments on folding in spreading-gliding nappes. Tectonophysics 145, 129–139.

Burliga, S., 1996. Kinematics within the Klodawa salt diapir, central Poland. In: Alsop, G.I., Blundell, D.J., Davison, I. (Eds.), Salt Tectonics. Geological Society Special Publication, vol. 100, pp. 11–21.

Carreras, J., Estrada, A., White, S., 1977. The effects of folding on the C-axis fabrics of a quartz mylonite. Tectonophysics 39, 3–24.

Carter, D.C., 1990a. Geology of the Canadian Salt Company Ltd. Pugwash Mine, 630 Level, Pugwash, Nova Scotia. Nova Scotia Department of Mines and Energy, Map 90–1.

Carter, D.C., 1990b. Geology of the Canadian Salt Company Ltd. Pugwash Mine, 730 Level, Pugwash, Nova Scotia. Nova Scotia Department of Mines and Energy, Map 90–2.

Carter, D.C., 1990c. Geology of the Canadian Salt Company Ltd. Pugwash Mine, 830 Level, Pugwash, Nova Scotia. Nova Scotia Department of Mines and Energy, Map 90–3.

Clarke, B.M., Uken, R., Watkeys, M.K., Reinhardt, J., 2005. Folding of the Rustenberg layered suite adjacent to the Steelpoort pericline: implications for syn-Bushveld tectonism in the eastern Bushveld Complex. South African Journal of Geology 108, 397–412.

Cobbold, P.R., Quinquis, H., 1980. Development of sheath folds in shear regimes. Journal of Structural Geology 2, 119–126.

Cox, P., 2006. The glaciotectonics of the North Norfolk coast. Unpublished B.Sc. thesis, University of St. Andrews.

Crispini, L., Capponi, G., 1997. Quartz fabric and strain partitioning in sheath folds: an example from the Voltri Group (Western Alps, Italy). Journal of Structural Geology 19, 1149–1157.

Davison, I., Bosence, D., Alsop, G.I., Al-Aawah, M.H., 1996. Deformation and sedimentation around active Miocene salt diapirs on the Tihama Plain, northwest Yemen. In: Alsop, G.I., Blundell, D.J., Davison, I. (Eds.), Salt Tectonics. Special Publications, vol. 100. Geological Society of London, pp. 23–39.

Decker, P.L., 1990. Style and mechanics of liquefaction-related deformation, lower Absaroka Volcanic Supergroup (Eocene), Wyoming. In: Special Paper, vol. 240. Geological Society of America, 71 pp.

Dubey, A.K., Cobbold, P.R., 1977. Noncylindrical flexural slip folds in nature and experiment. Tectonophysics 38, 223–239.

Escher, B.G., Kuenen, P.H., 1929. Experiments in connection with salt domes. Leidsche Geologische Mededeelingen 3, 82–151.

Eyles, N., Eyles, C.H., McCabe, A.M., 1989. Sedimentation in an ice-contact subaqueous setting: the mid-Pleistocene "North Sea drifts" of Norfolk, UK. Quaternary Science Reviews 8, 57–74.

Farrell, S.G., Eaton, S., 1987. Slump strain in the Tertiary of Cyprus and the Spanish Pyrenees. Definition of palaeoslopes and models of soft-sediment deformation. In: Jones, M.E., Preston, R.M.F. (Eds.), Deformation of Sediments and Sedimentary Rocks. Special Publications of the Geological Society of London, vol. 29, pp. 181–196.

Farrell, S.G., Eaton, S., 1988. Foliations developed during slump deformation of Miocene marine sediments, Cyprus. Journal of Structural Geology 10, 567–576.

Faure, M., 1985. Microtectonic evidence for eastward ductile shear in the Jurassic orogen of SW Japan. Journal of Structural Geology 7, 175–186.

Fowler, A.R., El Kalioubi, B., 2002. The Migif-Hafafit gneissis complex of the Egyptian Eastern Desert: fold interference patterns involving multiply deformed sheath folds. Tectonophysics 346, 247–275.

Ganesan, T.M., Gopalakrishnan, K., Renganathan, R., Sivasankaran, S.S., 1999. Sheath fold in Charnokite around Nekkanamalai, Vellore District, Tamil Nadu. Journal Geological Society of India 54, 69–72.

George, A., 1990. Deformation processes in an accretionary prism: a study from the Torlesse terrane of New Zealand. Journal of Structural Geology 12, 747–759.

Ghosh, S.K., 1993. Structural Geology: Fundamentals and Modern Developments. Pergamon Press, 598 pp.

Ghosh, S.K., Mukhopadhyay, A., 1986. Soft-sediment recumbent folding in a slump-generated bed in Jharia basin, Eastern India. Journal Geological Society of India 27, 194–201.

Ghosh, S.K., Ramberg, H., 1968. Buckling experiments on intersecting fold patterns. Tectonophysics 5, 89–105.

Ghosh, S.K., Sengupta, S., 1984. Successive development of plane noncylindrical folds in progressive deformation. Journal of Structural Geology 6, 703–709.

Goodsell, B., Hambrey, M.J., Glasser, N.F., 2002. Formation of band ogives and associated structures at Bas Glacier d'Arolla, Valais, Switzerland. Journal of Glaciology 48, 287–300.

Guilbaud, M.-N., Self, S., Thordarson, T., Blake, S., 2005. Morphology, surface structures, and emplacement of lavas produced by Laki, A.D. 1783–1784. In: Manga, M., Ventura, G. (Eds.), Kinematics and Dynamics of Lava Flows. Special Paper, vol. 396. Geological Society of America, pp. 81–102.

Hanmer, S., Hamilton, M.A., Crowley, J.L., 2002. Geochronological constraints on Paleoarchean thrust-nappe and Neoarchean accretionary tectonics in southern West Greenland. Tectonophysics 350, 255–271.

Hansen, E., 1971. Strain Facies. Springer-Verlag, New York, 207 pp.

Harland, W.B., Mann, A., Townsend, C., 1988. Deformation of anhydrite-gypsum rocks in central Spitsbergen. Geological Magazine 125, 103–116.

Harms, T.A., Burger, H.R., Blednick, D.G., Cooper, J.M., King, J.T., Owen, D.R., Lowell, J., Sincock, M.J., Kranenburg, S.R., Pufall, A., Picornell, C.M., 2004. Character and origin of Precambrian fabrics and structures in the Tobacco Root Mountains, Montana. In: Brady, J.B., Burger, H.R., Cheney, J.T., Harms, T.A. (Eds.), Precambrian Geology of the Tobacco Root Mountains, Montana. Special Paper, vol. 377. Geological Society of America, pp. 203–226.

Hart, J.K., 1997. The relationship between drumlins and other forms of subglacial glaciotectonic deformation. Quaternary Science Reviews 16, 93–107.

Henderson, J.R., 1981. Structural analysis of sheath folds with horizontal X-axes, northeast Canada. Journal of Structural Geology 3, 203–210.

Hibbard, J., Karig, D.E., 1987. Sheath-like folds and progressive fold deformation in Tertiary sedimentary rocks of the Shimanto accretionary complex, Japan. Journal of Structural Geology 9, 845–857.

Hippertt, J., 1999. Are S-C structures, duplexes and conjugate shear zones different manifestations of the same scale-invariant phenomenon? Journal of structural Geology 21, 975–984.

Hobbs, B.E., Myhlhaus, H-B., Ord, A., Zhang, Y., Moresi, L., 2000. Fold geometry and constitutive behaviour, in: Jessell, M.W., Urai, J.L. (Eds.), Stress, Strain and Structure, A Volume in Honour of W.D. Means. Journal of the Virtual Explorer, 2.

Hobbs, B., Regenauer-Lieb, K., Ord, A., 2007. Thermodynamics of folding in the middle to lower crust. Geology 35, 175–178.

Holdsworth, R.E., 1989. The geology and structural evolution of a Caledonian fold and ductile thrust zone, Kyle of Tongue region, Sutherland, N. Scotland. Journal of the Geological Society of London 146, 809–823.

Holdsworth, R.E., 1990. Progressive deformation structures associated with ductile thrusts in the Moine Nappe, Sutherland, N. Scotland. Journal of Structural Geology 12, 443–452.

Hoy, R.B., Foose, R.M., O'Neill, B.J., 1962. Structure of Winnfield salt dome, Winn Parish, Louisiana. American Association of Petroleum Geologists Bulletin 46, 1444–1459.

Hudleston, P., 1992. A comparison between glacial movement and thrust sheet or nappe emplacement and associated structures. In: Mitra, S., Fisher, G.W. (Eds.), Structural Geology of Fold and Thrust Belts. The Johns Hopkins University Press, pp. 81–93.

Jackson, M.P.A., Talbot, C.J., 1989. Anatomy of mushroom-shaped diapirs. Journal of Structural Geology 11, 211–230.

Jackson, M.P.A., Cornelius, R.R., Craig, C.H., Gansser, A., Stocklin, J., Talbot, C.J., 1990. Salt diapirs of the Great Kavir, Central Iran. Geological Society of America Memoir 177, 1–139.

Jackson, M.P.A., Scultz-Ela, D.D., Hudec, M.R., Watson, I.A., Porter, M.L., 1998. Structure and evolution of upheaval dome: a pinched-off salt diapir. Geological Society of America Bulletin 110, 1547–1573.

Jacobson, H.P., Waddington, E.D., 2004. Recumbent folding in ice sheets: a core referential study. Journal of Glaciology 50, 3–16.

Kelly, N.M., Clarke, G.L., Carson, C.J., White, R.W., 2000. Thrusting in the lower crust: evidence from the Oygarden Islands, Kemp Land, East Antarctica. Geological Magazine 137, 219–234.

Kent, P.E., 1970. The salt plugs of the Persian Gulf region. Transactions of the Leicester Literary and Philosophical Society 64, 56–88.

Kluiving, S.J., Rappol, M., Van der Wateren, D., 1991. Till stratigraphy and ice movements in eastern Overijssel, The Netherlands. Boreas 20, 193–205.

Kuiper, Y.D., Jiang, D., Lin, S., 2007. Relationship between non-cylindrical fold geometry and the shear direction in monoclinic and triclinic shear zones. Journal of Structural Geology 29, 1022–1033.

Kupfer, D.H., 1962. Structure of Morton Salt Company mine, Weeks Island salt dome, Louisiana. American Association of Petroleum Geologists Bulletin 46, 1460–1467.

Kupfer, D.H., 1976. Shear zones inside Gulf Coast salt stocks help to delineate spines of movement. American Association of Petroleum Geologists Bulletin 60, 1434–1447.

Lacassin, R., Mattauer, M., 1985. Kilometre-scale sheath fold at Mattmark and implications for transport direction in the Alps. Nature 315, 739–742.

Lian, O.B., Hicock, S.R., Dreimanis, A., 2003. Laurentide and Cordilleran fast ice flow: some sedimentological evidence from Wisconsinan subglacial till and its substrate. Boreas 32, 102–113.

Liu, J., Liu, Y., Chen, H., Sha, D., Wang, H., 1997. The inner zone of the Liaoji Paleorift: its early structural styles and structural evolution. Journal of Asian Earth Sciences 15, 19–31.

Malavieille, J., Ritz, J.F., 1989. Mylonitic deformation of evaporites in decollements: examples from the Southern Alps, France. Journal of Structural Geology 11, 583–590.

Maltman, A., 1994. Deformation structures preserved in rocks. In: Maltman, A. (Ed.), The Geological Deformation of Sediments. Chapman and Hall, pp. 261–307.

Marcoux, J., Brun, J.-P., Burg, J.-P., Ricou, L.E., 1987. Shear structures in anhydrite at the base of thrust sheets (Antalya, Southern Turkey). Journal of Structural Geology 9, 555–561.

Marques, F.G., Cobbold, P.R., 1995. Development of highly non-cylindrical folds around rigid inclusions in bulk simple shear regimes: natural examples and experimental modelling. Journal of Structural Geology 17, 589–602.

Matoshko, A.V., 1995. The Dnieper Glaciation: bedrock dislocations and glacial erosional landscapes. In: Ehlers, J., Kozarski, S., Gibbard, P. (Eds.), Glacial Deposits in North-East Europe. A.A. Balkema, Rotterdam, Netherlands, pp. 241–248.

McBride, E.F., 1962. Flysch and associated beds of the Martinsburg Formation (Ordovician), Central Appalachians. Journal of Sedimentary Petrology 32, 39–91.

McCaffrey, K.J.W., Grocott, J., Garde, A., Thrane, K., Hand, M. Connelly, J., 2006. An exposed channel flow structure in the northern Nagssugtoqidian-Rinkian collisional system, West Greenland. Abstract. Tectonic Studies Group, Manchester, 3–6 January 2006, p. 59.

Merschat, A.J., Hatcher, R.D., Davis, T.L., 2005. The northern Inner Piedmont, southern Appalachians, USA: kinematics of transpression and SW-directed mid-crustal flow. Journal of Structural Geology 27, 1252–1281.

Mies, J.W., 1993. Structural analysis of sheath folds in the Sylacauga Marble Group, Talladega slate belt, southern Appalachians. Journal of Structural Geology 15, 983–993.

Miller, J., McL, Gray, D.R., Gregory, R.T., 2002. Geometry and significance of internal windows and regional isoclinal folds in northeast Saih Hatat, Sultanate of Oman. Journal of Structural Geology 24, 359–386.

Minnigh, L.D., 1979. Structural analysis of sheath folds in a meta-chert from the western Italian Alps. Journal of Structural Geology 1, 275–282.

Möller, P., 2006. Rogen moraine: an example of glacial reshaping of preexisting landforms. Quaternary Science Reviews 25, 362–389.

Muehlberger, W.R., Clabaugh, P.S., 1968. Internal structure and petrofabrics of Gulf coast salt domes. In: Braunstein, J., O'Brien, G.D. (Eds.), Diapirism and Diapirs. American Association of Petroleum Geologists Memoir, vol. 8, pp. 90–98.

Mulugeta, G., Koyi, H., 1987. Three dimensional geometry and kinematics of experimental piggyback thrusting. Geology 15, 1052–1056.

Nigro, F., Renda, P., 2004. Growth pattern of underlithified strata during thrust-related folding. Journal of Structural Geology 26, 1913–1930.

Orozco, M., Alvarez-Valero, A.M., Alonso-Chaves, F.M., Platt, J.P., 2004. Internal structure of a collapsed terrain The Lujar syncline and it's significance for the fold- and sheet-structure of the Alboran Domain (Betic Cordilleras, Spain). Tectonophysics 385, 85–104.

Owen, L.A., 1988. Wet-sediment deformation of Quaternary and recent sediments in the Skardu Basin, Karakoram Mountains, Pakistan. In: Croot, D.G. (Ed.), Glaciotectonics: Forms and Processes. Balkema, Rotterdam, pp. 123–147.

Owen, L.A., Derbyshire, E., 1988. Glacially deformed diamictons in the Karakoram Mountains, northern Pakistan. In: Croot, D.G. (Ed.), Glaciotectonics: Forms and Processes. Balkema, Rotterdam, pp. 149–176.

Pedersen, S.A.S., 2000. Superimposed deformation in glaciotectonics. Bulletin of the Geological Society of Denmark 46, 125–144.

Piotrowski, J.A., Windelberg, S., 2003. Glazialtektonik weichselzeitlicher Ablagerungen in Zentral Fünen Dänemark. Eiszeitalter und Gegenwart 53, 39–53.

Platt, J.P., Lister, G.S., 1985. Structural evolution of a nappe complex, southern Vanoise massif, French Penninic Alps. Journal of Structural Geology 7, 145–160.

Price, N.J., Cosgrove, J.W., 1990. Analysis of geological structures. Cambridge University Press, Cambridge, 502 pp.

Quane, S.L., Russell, J.K., 2005. Ranking welding intensity in pyroclastic deposits. Bulletin of Volcanology 67, 129–143.

Quinquis, H., Audren, C., Brun, J.P., Cobbold, P., 1978. Intensive progressive shear in Ile de Groix blueschists and compatibility with subduction or obduction. Nature 274, 43–45.

Ramberg, H., 1963. Fluid dynamics of viscous folding. American Association of Petroleum Geologists Bulletin 47, 484–515.

Ramsay, J.G., 1967. Folding and Fracturing of Rocks. McGraw-Hill, New York, 568 pp.

Ramsay, J.G., 1980. Shear zone geometry: a review. Journal of Structural Geology 2, 83–99.

Ramsay, J.G., 1982. Rock ductility and its influence on the development of tectonic structures in mountain belts. In: Hsu, K.J. (Ed.), Mountain Building Processes. Academic Press, pp. 111–127.

Ramsay, J.G., Huber, M.I., 1987. Folds and Fractures. In: The Techniques of Modern Structural Geology, vol. 2. Academic Press.

Rhodes, S., Gayer, R.A., 1977. Non-cylindrical folds, linear structures in the X-direction and mylonite developed during translation of the Caledonian Kalak Nappe Complex of Finnmark. Geological Magazine 114, 329–341.

Roberts, A., 1989. Fold and thrust structures in the Kintradwell "boulder beds", Moray Firth. Scottish Journal of Geology 25, 173–186.

Roberts, W., Williams, P.F., 1993. Evidence for early Mesozoic extensional faulting in Carboniferous rocks, southern New Brunswick, Canada. Canadian Journal of Earth Sciences 30, 1324–1331.

Rosas, F.M., Marques, F.O., Luz, A., Coelho, S., 2002. Sheath folds formed by drag induced by rotation of rigid inclusions in viscous simple shear flow: nature and experiment. Journal of Structural Geology 24, 45–55.

Rowe, C.D., Moore, J.C., Meneghini, F., McKeirnan, A.W., 2005. Large-scale pseudotachylytes and fluidised cataclasites from an ancient subduction thrust fault. Geology 33, 937–940.

Salinas-Prieto, J.C., Monod, O., Faure, M., 2000. Ductile deformations of opposite vergence in the eastern part of the Guerrero Terrane (SW Mexico). Journal of South American Earth Sciences 13, 389–402.

Sans, M., Sanchez, A.L., Santanach, P., 1996. Internal structure of a detachment horizon in the most external part of the Pyrenean fold and thrust belt (northern Spain). In: Alsop, G.I., Blundell, D.J., Davison, I. (Eds.), Salt Tectonics. Geological Society Special Publication, vol. 100, pp. 65–76.

Sarr, R., Ndiaye, P.M., Niang-Diop, I., Gueye, M., 2000. Datation by planktonic foraminiferas of a Lutetian volcanic activity in Toubab Dialaw (western Senegal). Bulletin Societé Géologique de France 171, 197–205.

Schoonver, M., Osozawa, S., 2004. Exhumation process of the Nago subduction-related metamorphic rocks, Okinawa, Ryukyu island arc. Tectonophysics 393, 221–240.

Searle, M.P., Alsop, G.I., 2007. Eye to eye with a mega-sheath fold: a case study from Wadi Mayh, northern Oman Mountains. Geology 35, 1043–1046.

Seno, S., Dallagiovanna, G., Vanossi, M., 1998. From finite strain data to strain history: a model for a sector of the Ligurian Alps, Italy. Journal of Structural Geology 20, 573–585.

Shao, J., Fu, Y., Zang, Q., Wang, Y., 1989. Ductile instability – Shentangyu ductile shear zone and tremolite glass in Huairou, Beijing. Physics and Chemistry of the Earth 17, 39–44.

Simpson, C., De Paor, D.G., 1993. Strain and kinematic analysis in general shear zones. Journal of Structural Geology 15, 1–120.

Skjernaa, L., 1989. Tubular folds and sheath folds: definitions and conceptual models for their development, with examples from the Grapesvare area, northern Sweden. Journal of Structural Geology 11, 689–703.

Smith, J.V., 2000. Flow pattern within a Permian submarine slump recorded by oblique folds and deformed fossils, Ulladulla, south-eastern Australia. Sedimentology 47, 357–366.

Strachan, L.J., Alsop, G.I., 2006. Slump folds as estimators of palaeoslope: a case study from the Fisherstreet Slump of County Clare, Ireland. Basin Research 18, 451–470.

Talbot, C.J., Aftabi, P., 2004. Geology and models of salt extrusion at Qum Kuh, central Iran. Journal of the Geological Society, London 161, 321–334.

Talbot, C.J., Jackson, M.P.A., 1987. Internal kinematics of salt diapirs. American Association of Petroleum Geologists Bulletin 71, 1068–1093.

Talbot, C.J., Koyi, H., 1998. An active nappe in Neoproterozoic rock salt. In: Snoke, A.W., Tullis, J., Todd, V.R. (Eds.), Fault-Related Rocks: A Photographic Atlas. Princeton University Press, Princeton, NJ, pp. 556–557.

Theunissen, K., Smirnova, L., Dehandschutter, B., 2002. Pseudotachylytes in the southern border fault of the Cenozoic intracontinental Teletsk basin (Altai, Russia). Tectonophysics 351, 169–180.

Thomas, G.S.P., 1984. The origin of the glacio-dynamic structure of the Bride Moraine, Isle of Man. Boreas 13, 355–364.

Van der Pluijm, B.A., 1986. Geology of eastern New World Island, Newfoundland: an accretionary terrane in the northeastern Appalachians. Geological Society of America Bulletin 97, 932–945.

Van der Wateren, F.M., 1999. Structural geology and sedimentology of the Heiligenhafen till section, Northern Germany. Quaternary Science Reviews 18, 1625–1639.

Van der Wateren, F.M., Kluiving, S.J., Bartek, L.R., 2000. Kinematic indicators of subglacial shearing. In: Maltman, A.J., Hubbard, B., Hambrey, M.J. (Eds.), Deformation of Glacial Materials. Special Publications, vol. 176. Geological Society London, pp. 259–278.

Vollmer, F.W., 1988. A computer model of sheath-nappes formed during crustal shear in the Western Gneiss Region, central Norwegian Caledonides. Journal of Structural Geology 10, 735–743.

Wang, G., Jiang, B., Yu, Z., 1994. Sheath folds formed under the action of gliding nappe and shearing. Chinese Science Bulletin 39, 1463–1467.

Webb, B.C., Cooper, A.H., 1988. Slump folds and gravity slide structures in a lower Palaeozoic marginal basin sequence (the Skiddaw Group), NW England. Journal of Structural Geology 10, 463–472.

Weijermars, R., 1997. Principles of Rock Mechanics. Alboran Science Publishing Ltd, 360 pp.

Williams, P.F., Zwart, H.J., 1977. A model for the development of the Seve-Koli Caledonian nappe complex. In: Saxena, S.K., Bhattacharji, S. (Eds.), Energetics of Geological Processes. Springer-Verlag, New York, pp. 169–187.